

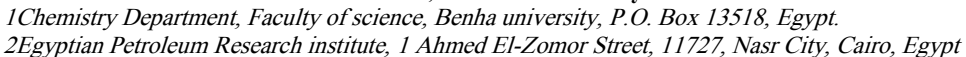
Egyptian Journal of Chemistry

http://ejchem.journals.ekb.eg/



Guar Gum-Neem Gum Antimicrobial Biofilms for Preservation of Biological Samples

Ahmed E. Elhassany¹, Iman A. Gadelkarim¹, Mohamed S. Behalo¹, Manar El-Sayed Abdel-Raouf², Mohamed Keshawy²





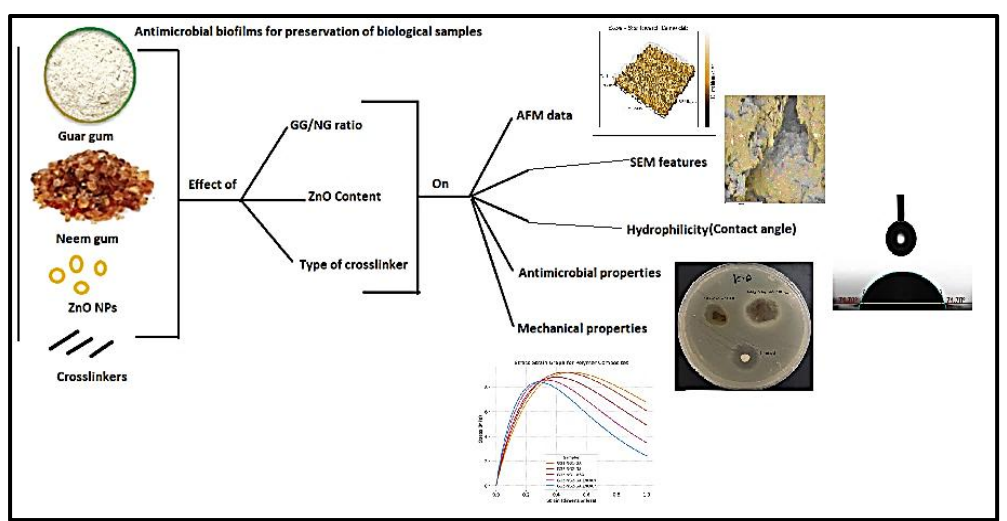
Abstract

This study reports the preparation and comprehensive characterization of five biodegradable biofilms made up from crosslinked guar gum (GG) and neem gum (NG), reinforced with zinc oxide nanoparticles (ZnO NPs). The biofilms were fabricated using thermal crosslinking with two different crosslinkers: glutaraldehyde (GA) and N,N'-methylenebisacrylamide (MBA). ZnO NPs were added at two loadings (0.5% and 0.7%) to improve mechanical strength and antimicrobial activity. The films were coded according to their GG/NG ratio, crosslinker type, and ZnO content. Structural and morphological analyses were carried out using FTIR, AFM, SEM, and EDX mapping. FTIR confirmed successful crosslinking and ZnO incorporation. AFM and SEM results showed that surface roughness and topography varied notably with the GG/NG ratio, crosslinker type, and ZnO loading. The GG₂-NG₁-GA film exhibited the smoothest surface with the lowest roughness values. EDX mapping verified the uniform distribution of ZnO NPs in the relevant samples. The mechanical tests showed that the tensile strength of the films ranged from 3.2 to 7.5 MPa, with GG₂-NG₁-GA achieving a balanced strength of about 5 MPa and good flexibility, making it suitable for packaging applications. Water solubility and water vapor permeability tests confirmed that the GG2-NG1-GA film had the highest solubility and water holding capacity among all formulations. Antimicrobial testing demonstrated effective inhibition of six pathogenic microorganisms, although Aspergillus niger showed resistance, indicating a need for further antifungal enhancement. Overall, the results highlight the potential of these GG-NG biofilms, especially GG₂-NG₁-GA, as eco-friendly materials for preserving biological samples due to their balanced mechanical properties, good flexibility, and antimicrobial performance.

Keywords:

Antimicrobial activity, mechanical properties, biofilms, biological samples, Guar gum, Neem gum, ZnO NPs.

Graphical abstract:



1. Introduction

The preservation of biological samples—such as tissues, cells [1,2], and biofluids such as blood and semen [1,3] is critical for biomedical research, diagnostics, and biobanking and tracking crimes[4-6]. The proper preservation of these samples is very important especially when crimes are committed against an unknown person, as it is necessary to preserve evidence in good condition for a period of time until new evidence or developments emerge that require reopening the investigation [4,7]. Therefore, maintaining sample integrity during storage requires stringent control over environmental factors like moisture, oxygen, and microbial contamination, which can degrade biomolecules and compromise downstream analyses[6,8]. While conventional storage methods (e.g., cryopreservation or desiccants) are widely used, they often lack scalability or fail to provide long-term stability. Advanced packaging materials that actively regulate the sample microenvironment could address these limitations [9]. Interestingly, the food industry has pioneered similar challenges in preserving perishable goods, where barrier films, oxygen scavengers, and antimicrobial coatings are routinely employed to extend shelf life. These technologies, though designed for food, share fundamental principles with biological preservation—such as mitigating oxidative damage and microbial growth—and may offer adaptable solutions for biomedical applications [10-13]. From the historical point of view, some plant exudates and gums were used in preservation of biological bodies [14]. For instance, Ancients Egyptian used several natural and plant-based materials such as Natron salt, Coniferous resin, Mastic, Myrrh, Beeswax, Bitumen, Cassia, Onions, Lichen, Henna and Gum Arabic for mummification [15]. After the exploration and production of petroleum crude oil, the synthetic and petroleum-based polymers have been widely utilized as packaging materials due to their acceptable mechanical and thermal properties [16]. However, the continuous use of these non-biodegradable materials over years have caused a lot of ecological impacts due to their long-standing in the environment [17]. Recently, environmental awareness has augmented towards the employment of eco-friendly, renewable, and biodegradable staffs for sustainable packaging applications [18,19]. These polymers include cellulose [20], chitosan [21][22] and starch [23]. However, the challenge of weak mechanical properties and high- water permeability is a chief disadvantage that restricts the application of natural polymers in packaging [24]. Several investigators suggested different modification protocols to manipulate these drawbacks. These include derivatization [25-27], crosslinking [28-30] and fabrication with inorganic materials [23,31-33]. On the other hand, guar gum -Figure 1a- (a carbohydrate polymer composed of linear chain of 1, 4-linked D-mannose units with 1,6-linked galactose units grafted as a single side-chain) is one of the most commonly used polymers in different environmental applications due to its high functionality and facile adaptability [34][35]. In this regard, groundnut husk modified with Guar Gum was harnessed for the absorptive removal of some cations (Pb2+, Cu2+ and Ni2+) from aqueous solution [36]. Also, Magnetic guar gum nanocomposites were used for catalytic reduction of p-nitroaniline [37]. In another work, Congo red dye was encapsulated in carboxymethyl guar gum – Alginate gel microspheres [38]. However, the utilization of modified guar gum in packaging applications was widely addressed. In this respect, Arfat et al [39] investigated the potential of gum/Ag-Cu nanocomposite films as an active food packaging material. In addition, green chemistry modification was conducted to prepare hydrophobically modified guar gum (HMG) via microwave assisted condensation with a dimer of ricinoleic acid derived from castor oil. The condensation product was then merged with polyvinyl alcohol and casted into green films for packaging applications [39,40]. In order to improve the mechanical properties of guar gum products, some inorganic fillers can be added. For packaging purposes, it is highly advantageous to incorporate inorganic fillers with proved antimicrobial activity such as zinc oxide nanoparticles, silver nanoparticles, titanium nanoparticles...etc [41]. On the other hand, active packaging materials with established antimicrobial activity are highly requested in food preservation. They can be prepared by incorporation of active ingredients such as essential oils (Clove oil, tea tree oil...etc) [42] and/or plant extract (Cinnamon, curcumin...etc) [43]. On the other hand, Neem plant (Melia azadirachta, Meliaceae) is cultivated in India and Myanmar and known as the village pharmacy due to its outstanding therapeutic potential and antimicrobial activity induced by several active materials that can be obtained from all the parts of the plant [44]. Earlier studies have proved the antimicrobial activity of neem extract towards Aspergillus parasiticus [45], Candida albicans [46], Staphylococcus aureus, Escherichia coli, Pseudomonas aeruginosa and Candida albicans [47], Aspergillus flavus [48], common dermatophytes [49] Aspergillus flavus, Aspergillus fumigatus, Aspergillus niger, Aspergillus terreus, Candida albicans and Microsporum gypseum) [50]. Recently, several research works investigated the antimicrobial effect of modified neem extracts. In this regard, the antibacterial activity of neem extract and its silver nanoparticles was investigated against Pseudomonas aeruginosa [51]. In another work, Kaur et al studied the antimicrobial and anti-Inflammatory action of low-energy assisted nanohydrogel of Azadirachta indica [52]. In this work, neem gum as a common plant exudate was used as a neem product to induce the antimicrobial activity of the biofilms. Chemically, it is the salt of a complex polysaccharide acid, Figure 1b.

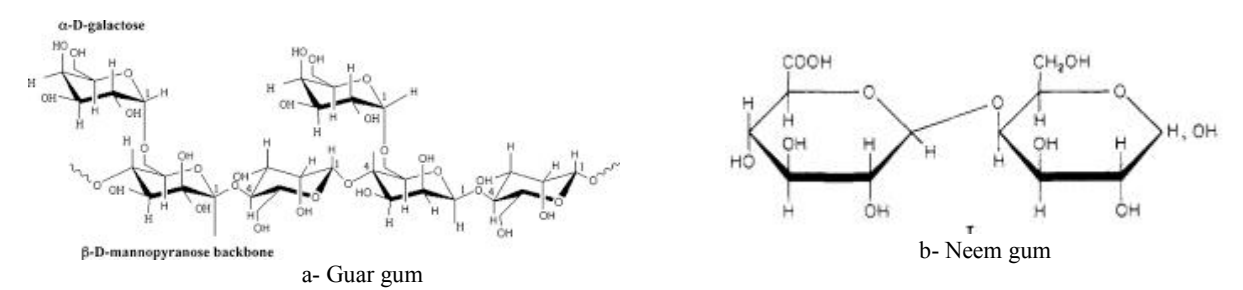


Fig. 1. Chemical structures of guar gum and neem gum

On the other hand, plasticizers are probably required in the manufacture of the biopolymers-based films to impart plastic properties and to reduce the undesirable brittleness on the resultant film [53]. The plasticizers must be uniformly dispersed in the polymer matrix to assist in the slide of polymer chain, thereby refining the toughness and flexibility of the film [41]. The commonly known plasticizers used for the fabrication of films include-but not limited to- glycerol, sorbitol, ethylene glycol, and propylene glycol [54]. They are usually used when the components of the membranes are rigid.

In the present work, the advantageous features of guar gum and neem gum were combined to prepare several crosslinked biofilms (applying two crosslinkers) with potent antimicrobial properties for preservation of biological samples of different types. Aiming to enhance the antimicrobial activity, zinc oxide nanoparticles were added to some membranes. Generally, variation in the composition of the as-prepared biofilms targets the following variables:

- 1- Effect of guar gum/neem ratio.
- 2- Effect of zinc oxide ratio.
- 3- Effect of type of crosslinker.

However, the prepared biofilms were characterized for their composition (FTIR spectroscopy and thermal stability), their morphology and topographies (SEM and AFM) and their performance (contact angle, mechanical properties, antimicrobial properties and water permeability features). The content of zinc oxide was assessed in some films via EDX. The data obtained from this study was carefully interpreted in order to reach an optimized formulation for a model biofilm used in safeguarding different biological samples for long time.

2. Materials and methods:

2.1. Materials:

Ultra-pure guar gum powder (GG) with molecular weight of 2.5x105 g/mol was obtained from Sigma-Aldrich as yellowish white powder and used without further processing. Neem gum (NG) was obtained from a local herbalist store in Cairo in the form of powder. The powder was purified as mentioned in section (2.2.1.). Crosslinkers (Glutaraldehyde (GA) and Methylene bisacrylamide (MBA)) were obtained as analytical reagents from Fluka. Other chemicals such as ammonium persulfate (APS) and Zinc oxide nanoparticles (ZnO NPs) with average particle size 50-75 nm were obtained from El-Nasr Company for chemicals, Cairo, Egypt. Distilled water was used throughout the experimental steps.

2.2. Methods and preparations:

2.2.1. Purification of neem powder (NG):

In this step, 100 g of neem gum (NG) was dispersed in 500 ml distilled water via sonication for 30 minutes till obtaining homogeneous dispersion. Then, the dispersion was heated at 40 °C for 1 h and held aside for 2 h to settle. The solution was filtered and 500 ml of ethanol was added to the filtrate and kept in the refrigerator for 24 h at 8–10 °C. Later, purified NG was recovered by filtration, dried and stored in clean plastic bags.

2.2.2. Preparation of Guar Gum- Neem Gum crosslinked membrane:

The preparation of Guar Gum-Neem Gum membranes involves a two- step protocol to mix the components and to cast different polymer composites into a membrane form. Below is a general procedure that can guide the preparation of these composite membranes.

2.2.2.1. Preparation of Crosslinked Guar Gum/Neem Gum composite (GG-NG)

Firstly, Guar Gum and neem gum solutions (solution 1 and 2 respectively) were prepared by separately dissolving 1 gm of each gum in 100 ml of distilled water with efficient stirring to obtain 1% clear solution of each gum. Afterwards, the desired ratios (in weight percentage) were mixed with continuous stirring for two hours according to the amounts given in Table 1. Then, 0.5 g of APS was added to the blended solution with continuous stirring at 60oC to promote radical generation. Afterwards, 5 % of the crosslinker (either MBA or GA) was added into the new guar gum- neem gum solution. The new solution was stirred continuously for 6 hours at 80 oC until a homogeneous thick jelly-like solution was obtained. The solution was poured as a homogenous layer in a clean dry petri dish and placed in an air oven at 50 oC for post-curing. The membranes obtained at this step were coded as following: GG2-NG1-GA, GG2-NG2-GA and GG2-NG1-MBA.

2.2.2.2. Preparation of reinforced GG-NG composites:

In this step, ZnO nanoparticles were added into some formulations in order to explore the synergistic antimicrobial effect with neem gum. The incorporation of ZnO typically followed the mixing of two gums together. The solution was sonicated for 30 minutes to assure homogenous dispersion of the nanoparticles in the bulk of the solution before being heated. Then, the steps were repeated as in the previous section. The samples at this step were coded as: GG2-NG2-GA-ZnO0.5 and GG2-NG2-GA-ZnO0.7.

The codes and compositions of all samples are given in **Table 1**. It is worth mentioning that the preparation protocol is carefully designed to investigate the following effects:

- 1- 1 Effect of guar gum/neem ratio: Samples GG2-NG1-GA and GG2-NG2-GA (directly compare how the ratio of these natural polymers influences material properties, with all other variables held constant).
- 2- Effect of zinc oxide ratio: GG2-NG2-GA-ZnO0.5 and GG2-NG2-GA-ZnO0.7 (to evaluate the impact of ZnO loading (0.5% vs. 0.7%) on antimicrobial activity and barrier performance.
- 3- Effect of crosslinker: GG2-NG1-GA and GG2-NG1-MBA (probes how crosslinker chemistry affects mechanical stability and hydration resistance).

Table 1: Codes and Composition of the prepared bio-membranes

Code*	GG.	NG	GA	MBA	APS**	ZnO NPs
GG2-NG1-GA	2	1	5		0.5	
GG2-NG2-GA	2	2	5		0.5	
GG2-NG1-MBA	2	1		5	0.5	
GG2-NG2-GA-ZnO0.5	2	2	5		0.5	0.5
GG2-NG2-GA-ZnO0.7	2	2	5		0.5	0.7

^{*}The amount of materials in this table was calculated in weight %.

2.3. Characterizations:

- The chemical modification was confirmed by Fourier transform-infrared spectroscopy (Bruker, Unicom infra-red spectrophotometer, Germany) 400-4000 cm-1 wavelength range at room temperature using KBr disc method.
- Scanning electron microscope (SEM), model (JSM-7610F) was used to assess the morphology of the samples.
- The content of zinc oxide was assessed in some films via EDX, model (Bruker-ALPHA 2, Bruker Corporation, USA).
- The surface features and height measurements of the dry and loaded composites were assessed by AFM, model Flexaxiom Nanosurf, C3000 applying the dynamic mode (non-contact) with a silicon cantilever with a vibration frequency of 25kHz.
- The water contact angle (WCA) measurements were conducted using a VCA Video Contact Angle System (Krüss DSA25B, Germany) to evaluate the hydrophilicity of the biofilm surfaces.
- Elasticity and Tensile performance of the membranes were measured on a universal testing machine (CMT6502, Shenzhen SANS Test Machine Co. Ltd., China) with a tensile rate of 5 mm/min according to ISO6239-1986 to gain tensile strength and elongation at break. The mean values of tensile strength and elongation at break were attained from five replications.

2.4. Antibacterial activity:

The antimicrobial activities of GG2-NG1-GA, GG2-NG2-GA, GG2-NG1-MBA and GG2-NG2-GA-ZnO0.7 was assessed by the agar well diffusion method. In these experiments nutritional agar was used as a nourishing medium for the bacterial strains from the MTCC and the clinical strain of extended spectrum beta-lactamase (ESBL) at 4 °C. Microbial suspension (0.1%) of Candida albikans, Asp. Niger, S. aureus, E. coli, Bacillus subtilis and Klebsiella pneumonia were homogeneously spread on Muller-Hinton agar. The green composites (pieces 1cm x 1cm) were loaded into bores (6 mm diameter) and subjected to incubation at 37 °C for 24 hours. The observed diameter of the inhibition zone was recorded in mm. The data are given in the discussion section.

2.5. Determination of physical properties of films

2.5.1. Water Solubility (WS)

Water solubility (WS) was studied with the method of Jafarzadeh, Alias [54]. Samples were cut to standard sizes (30 mm x 30 mm) and conditioned in a desiccator for three days in a silica gel. The samples were weighed, placed in 80 mL of distilled water, and agitated at 100 rpm for 1 h at room temperature. The film leftover was filtered with filter paper and dried at 60 oC in an oven until constant weight. The solubility of the films was estimated according to Equation (1), where Wi is the initial dry weight and Wf the final dried weight of the film.

Water Solubility (%) =Wi-Wf/Wix100 (1)

2.5.2. Water Holding capacity (WHC)

WHC was calculated via a facile methodology. In brief, film specimens (2 cm x 2 cm) were put into duplicate and then they were dried in an electric oven, for 24 hours at 90 °C. The following formula was used to determine the moisture content value; Equation (2):

WHC(wt%) =
$$\frac{\text{mi-mf}}{\text{mf}} \times 100$$
 (2)

where mi and mf are the initial and final weights of film samples, respectively.

^{**} APS was added in weight percent.

2.5.3. Water vapor permeability (WVP)

A modified version of ASTM E96-95 was employed to determine the samples' water vapor permeability. A weighing vial held 3.0 g of pre-dried anhydrous calcium chloride. Next, the films were positioned at the bottle's top (its effective area measured (1.52×10-3 m2) and secured with elastic bands. The weighing bottles containing the film samples were then put inside a desiccator that contains a saturated solution of sodium chloride at the bottom (75% RH) and was kept at 25 °C. Over the course of 5 days, variations in the bottles' weight were reported to the nearest 0.000 gram at one day intervals. The watervapor transmission rate (WVTR) (g/day.m2) per unit of area was calculated using Eq. (3) and (slope) (g/day) was determined by linear regression.

WVTR =
$$\frac{\text{Slope}}{A} = \frac{\Delta m}{A \Lambda t}$$
 (3)

 $WVTR = \frac{Slope}{A} = \frac{\Delta m}{A\Delta t} \quad (3)$ where A is the area of the exposed film surface (1.52×10-3 m2), WVTR was measured in triplicates for each film sample.

2.6. Mechanical properties of the prepared biofilm

The mechanical properties of the prepared biofilms at different optimization conditions were measured. These included tensile strength (TS), elastic modulus (E), and elongation at break (EB) measurements of film samples at 25 °C and 53% relative humidity. Dumbbell-shaped specimens of 50 mm length and 4mm neck width at room temperature. The films were extended at 10 mm/min, and the analyses were performed with a 100 N load cell.

3. **Results and Discussion:**

3.1. Membrane preparation.

Guar gum-neem gum-ZnO composite membranes have emerged as a promising alternate for antimicrobial food packaging due to their biodegradable nature and potent bioactive properties [55]. Guar gum, a natural polysaccharide, provides excellent film-forming ability and flexibility, while neem gum contributes inherent antibacterial and antifungal properties, enhancing the film's protective function. The incorporation of zinc oxide (ZnO) nanoparticles further boosts antimicrobial activity, effectively inhibiting the growth of foodborne pathogens such as E. coli and S. aureus through mechanisms like reactive oxygen species (ROS) generation and membrane disruption [56]. These composite films exhibit improved mechanical strength, thermal stability, and barrier properties, making them suitable for extending shelf life and maintaining food quality [57]. Additionally, their eco-friendly composition aligns with sustainable packaging trends, consequently, reducing reliance on synthetic plastics. Several research works confirm their effectiveness against microbial contamination while remaining non-toxic for food contact applications [58,59]. With tunable properties through varying ZnO concentrations, these membranes offer a versatile, scalable, and green alternative for active packaging in the food and pharmaceutical industries [60]. A schematic illustration for the overall process followed in the preparation of Guar Gum-Neem gum-ZnO NPs biofilms is given in Fig. 2. The first step of reaction involved thermal degradation of APS into sulfate radicals which then combined with GG and NG to generate the macroradicals to form the crosslinked membranes with the aid of the applied crosslinker [61]. ZnO NPs were added as an inorganic reinforcing agent in some samples.

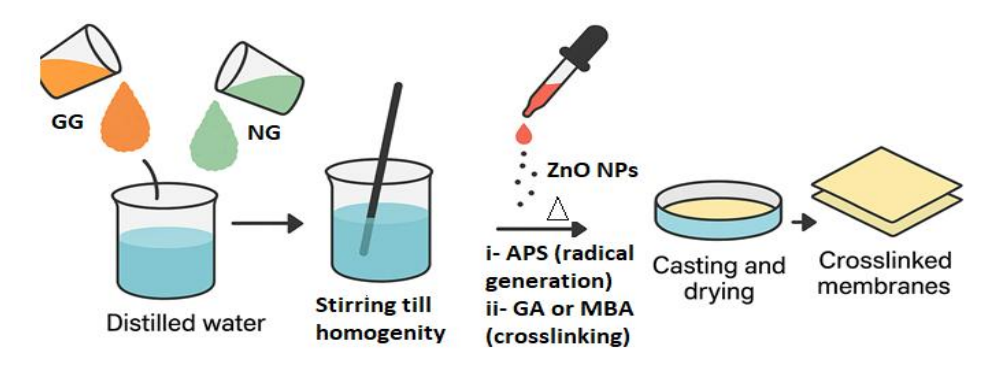


Fig. 2. Schematic illustration of preparation of Guar Gum-Neem gum-ZnO NPs biofilms

Verification of the chemical structure via the FTIR spectroscopy:

The FTIR spectra of [GG2-NG1-GA, GG2-NG2-GA and GG2-NG1-MBA] and [GG2-NG2-GA-ZnO0.5 and GG2-NG2-GA-ZnO0.7] are given in Fig.s 3 (I) and 3(II), respectively. The FTIR spectra demonstrated broad peak at 3300 -3460 cm⁻¹ due to O-H stretching from polysaccharides (present in both neem gum and guar gum). Besides attributable peaks have been found at 2920 cm⁻¹, 2840 cm⁻¹ corresponding to C-H stretching vibrations, 1700–1650 cm⁻¹ due to C=O stretching, 1400 cm⁻¹ corresponding to symmetric COO⁻ stretching. On the other hand, there are absorption bands at 1000–1100 cm⁻¹ attributed to C-O-C and C-O stretching (indicative of polysaccharide backbones) in addition to Zn-O stretching vibration

Egypt. J. Chem. 69, No. 2 (2026)

bands in the samples containing ZnO NPs at 814-600 cm⁻¹ [62]. However, differences in peak intensities, position and shape among the investigated samples suggest varying interactions strengths between the components. For example, stronger Zn–O peaks in the samples fabricated with ZnO might prove successful incorporation of ZnO. In addition, shifts or changes in the 1700–1000 cm⁻¹ range could point to chemical interaction or bonding between ZnO and the gum matrices. The most significant peaks in the FTIR spectrum of guar gum are typically associated with its polysaccharide structure, especially its hydroxyl and glycosidic groups. On the other hand, neem gum usually presents a more heterogeneous FTIR spectrum due to its complex mix of functionalities. The peaks of Guar gum are sharper and more polysaccharide-specific. An intense comparison between the most significant peaks in guar and neem gum are given in Table 2a. However, upon formation of guar gum-neem gum composites, several changes in peak location and intensity may occur due to the overlapping of functional groups or formation of hydrogen bonding between the O-H groups from guar gum and functional groups of neem gum, zinc oxide and the crosslinkers [61,63]. These changes are illustrated in Table 2b. Upon investigating the data provided in this table, several effects could be verified:

- Crosslinking Effect (GA): Stronger C=O and C=N related bands (~1728, ~1642 cm⁻¹) suggesting successful glutaraldehyde crosslinking in all samples containing GA as a crosslinker.
- Increasing Neem Gum (NG) ratio: No major shift in peak positions between GG2-NG1-GA, GG2-NG2-GA, but slight broadening of OH peak (3453 cm⁻¹) in GG2-NG2-GA implying more hydrogen bonding due to increased neem content.
- ZnO Addition (GG2-NG2-GA-ZnO0.5 and GG2-NG2-GA-ZnO0.7): Shifts/broadening in O–H and C=O regions (3392, 1728 cm⁻¹ and 3420, 1723, respectively) indicate interactions (likely H-bonding or coordination) between ZnO and hydroxyl/carbonyl groups. Also, broadened/split –OH and C=O regions suggest interaction with ZnO. Peaks at 946 and 814 cm⁻¹ may relate to Zn–O vibrations.
- Effect of improved crystallinity due to composite formation: Enhanced peaks in fingerprint region (1092, 1050, 883 cm⁻¹) suggest structural stabilization.
- Effect of type of crosslinker (MBA vs. GA Crosslinking):
 - o MBA (GG2-NG1-MBA) results in distinct amide I and II bands (1643, 1461 cm⁻¹), indicating covalent amide linkages.
 - GA (GG2-NG1-GA) leads to complex peaks around 1658–1625 cm⁻¹, reflecting Schiff base (C=N) and hydrogen bonding.

The overall conclusions reveal that GG2-NG2-GA-ZnO0.7 displays more complex interactions due to ZnO and GA, with signs of hydrogen bonding, and ZnO-matrix interaction; while GG2-NG1-MBA shows cleaner amide bands due to MBA crosslinking, more defined polymer structure, and absence of ZnO interference.

Table 2a: The most significant peaks in guar gum and neem gum according to their backbone

Wave number (cm ⁻¹)	Guar Gum	Neem Gum			
3453	Strong O–H stretch	Shows strong O–H with a different width			
2920, 2840	Aliphatic C–H	Often less intense than in guar gum			
1700–1650	Weak bending (moisture/uronic acid)	Strong band due to the C=O from numerous carboxyl groups			
1400	Symmetric COO ⁻ / CH ₂ bending	Often broader due to mixed functional groups			
1000-1100	Strong glycosidic band	May be less defined due to branched, heterogenous structure			

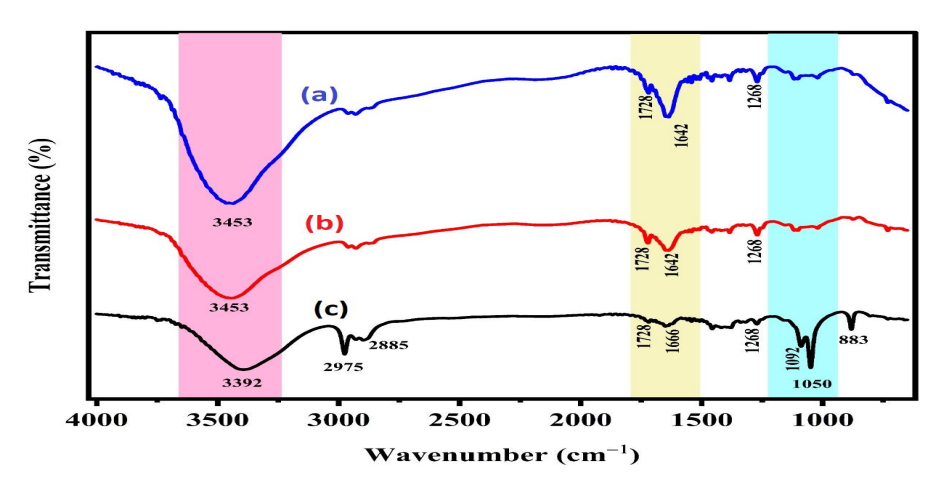


Fig. 3.(I): FTIR spectra of a- GG2-NG1-GA, b- GG2-NG2-GA and c-GG2-NG1-MBA

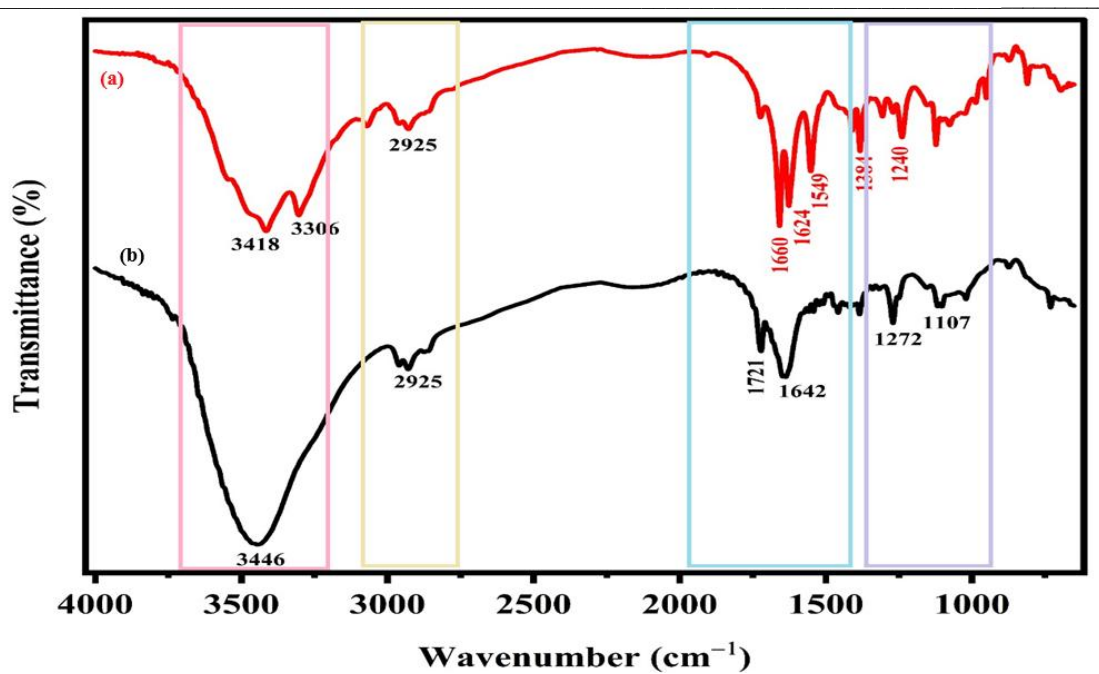


Fig. 3.(II): FTIR spectra of a- GG2-NG2-GA-ZnO0.5 and b- GG2-NG2-GA-ZnO0.7

Table 2b: Expected FTIR Features of Guar Gum-Neem Gum- ZnO Composites:

Wavenumber (cm ⁻¹)	Assignment	Observations
3453 / 3392	O-H stretching (hydroxyl groups)	Broad in all spectra; GG2-NG2-GA and GG2-NG1-GA similar; GG2-NG2-GA-ZnO0.5 slightly shifted due to ZnO-OH interaction.
3442	O-H and N-H stretching	In the spectrum of GG2-NG1-MBA indicating overlapped interaction
3420–3310	O-H and N-H stretching	In the spectrum of GG2-NG2-GA-ZnO0.7 shows more complex splitting (likely ZnO–OH and inter-H bonding)
2930, 3067 & 2927	C–H stretching	Aliphatic stretching in GG2-NG2-GA-ZnO0.7 and GG2-NG1-MBA with clearer separation in GG2-NG2-GA-ZnO0.7, possibly due to ZnO-induced ordering
1728	C=O stretching (aldehyde/carboxyl from GA or neem gum)	Appears in all the spectra with a slight shift in GG2-NG2-GA-ZnO0.5 indicating possible stronger interaction with ZnO.
1642 / 1666	H-O-H bending (bound water)	Present in samples but sharper in GG2-NG2-GA and GG2-NG2-GA-ZnO0.5 due to increased hydrogen bonding formation
1658–1625 and 1643	Amide I (C=O stretch in amide), or C=N (imine from GA), H-O-H bending	GG2-NG2-GA-ZnO0.7 shows multiple close peaks, possibly due to complex bonding (ZnO + GA); while and GG2-NG1-MBA shows a single peak at 1643 cm ⁻¹ indicating a stable amide.
1549 and 1461	Amide II (N–H bending), CH ₂ bending	In GG2-NG2-GA-ZnO0.7 and GG2-NG1-MBA Clear indication of amide formation in MBA-crosslinked sample (GG2-NG1-MBA)
1268	C–O bending / ether linkage	Present and nearly consistent in all the spectra due to the carbohydrate backbone of guar gum.
946, 814	Out-of-plane C-H bending, ZnO-related bands	Presence of ZnO possibly influences skeletal vibrations and shifts

3.3. AFM characterization:

The AFM was proved to be a very effective tool for surface characterization and topography monitoring [64,65]. In this regard, the AFM images of GG2-NG1-GA, GG2-NG2-GA, GG2-NG1-MBA, GG2-NG2-GA-ZnO0.5 and GG2-NG2-GA-ZnO0.7 are given in Fig.s 4a-e, respectively. Several factors are involved in shaping the surface features and controlling height values and roughness data given in Table 3a. These factors are as following:

- Effect of GG/NG ratio (Samples GG2-NG1-GA, GG2-NG2-GA): It can be seen that upon increasing the ratio of NG both height and roughness values increase accordingly, which may reflect higher interaction between the functional groups of both gums. In summary a higher neem gum content is expected to result in rougher, less uniform, and more textured surfaces in AFM images, due to the complex and branched nature of neem structure. The interpretation of these changes is summarized in Table 3b. These findings are in accordance to those mentioned by Bhardwaj et al [66].
- Effect of ZnO content (Samples GG2-NG2-GA-ZnO0.5 and GG2-NG2-GA-ZnO0.7): Incorporating zinc oxide (ZnO) nanoparticles into a polymeric matrix comprised of crosslinked GG/NG significantly alters the surface morphology and nanoscale features. Basically, low to moderate ZnO content caused an obvious increase in roughness and height, and introduced some nanodomains. These changes are interpreted in Table 3c. The effect of ZnO as an improver for barrier properties of biopolymer- Suberinic Acid Residues Films was studied by Jezo et al. They verified that addition of ZnO enhances the barrier properties of the prepared films [67].
- Effect of crosslinker (Samples GG2-NG1-GA, GG2-NG1-MBA): As outlined in Table 3d, the incorporation of GA resulted in lower height and smoother sample which fits membranes superior for barrier films requiring smoothness. On the other hand, incorporation of MBA resulted in highly porous membranes which are preferred for flexible packaging with superior mechanical properties [68].

Table 3a: AFM data of the investigated membranes

Biofilm code	Height (mean ± SD)	Ra (nm, mean ± SD)	n
GG2-NG1-GA	24.6 ± 2.1 nm	11.23 ± 1.5	3
GG2-NG2-GA	48.7 ± 3.8 nm	22.54 ± 2.3	3
GG2-NG1-MBA	252 ± 15 nm	40.4 ± 3.7	3
GG2-NG2-GA-ZnO0.5	157 ± 12 nm	34.11 ± 2.9	3
GG2-NG2-GA-ZnO0.7	$1.5 \pm 0.2 \; \mu m$	55.87 ± 4.1	3

Table 3b: Observable changes in AFM outcomes due to change in GG/NG ratio:

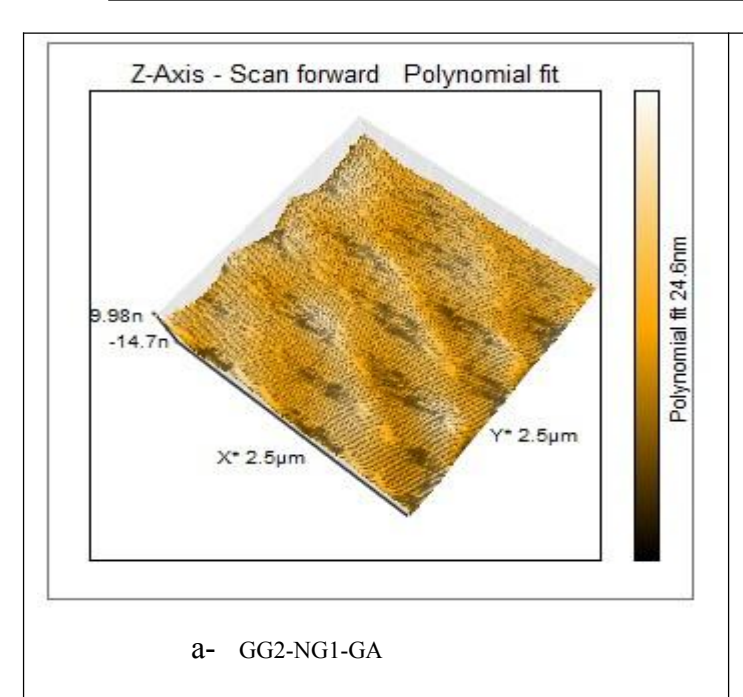
Tuble by Observable changes in 111 11 outcomes due to change in GO/1/G ratio.				
AFM feature	The current change	Explanation		
Topography	More irregular or granular	Neem gum has more functionalities than guar gum, introducing surface heterogeneity.		
Height	Increased average surface height	Bulky side groups in neem gum might induce micro-domains and height fluctuations. Also, they might cause more interaction with hydroxyl groups of GG.		
Roughness (Ra)	Higher roughness values	Greater intermolecular incompatibility and crosslinking variability can create nanoscale peaks and valleys.		
Homogeneity	Reduced	Guar gum is more uniform; neem gum introduces asymmetry and possible micro-or nano-aggregates.		

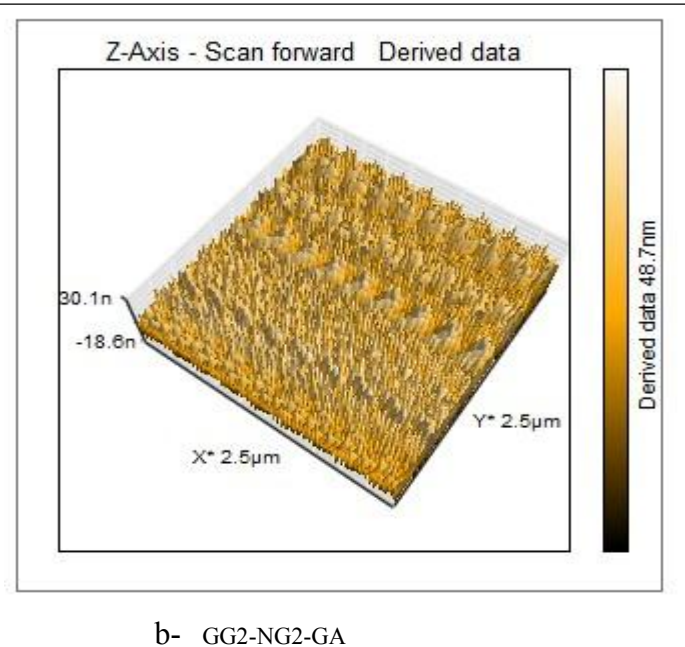
Table 3c: Current Effects of Changing ZnO Ratio on AFM Data:

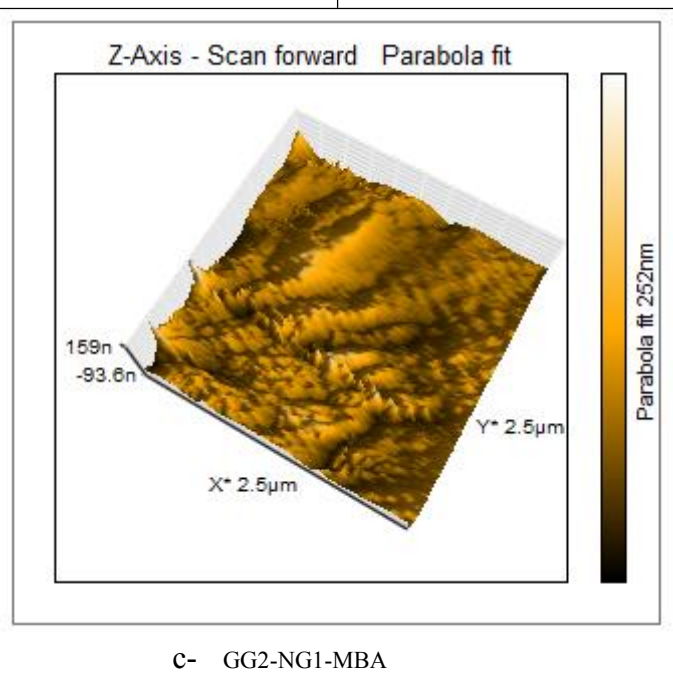
Table St. Culter Effects of Changing Zho Ratio on AFM Data.				
AFM feature	The current change	Explanation		
Topography	More defined particle-like features or clusters	ZnO particles can aggregate or embed in the polymer, forming raised domains.		
Height	Obvious increase	Surface height increases due to embedded nanoparticles or protrusions.		
Roughness (Ra)	Increases at moderate ZnO	Increasing ZnO increases roughness by disrupting the matrix.		
Nano-structuring	Potential creation of nanogaps or pores	Polymer-ZnO incompatibility results in phase separation.		

Table 3d: Effect of crosslinker on AFM findings

AFM Parameter	Glutaraldehyde (GA) Crosslinked GG-NG	Methylene Bisacrylamide (MBA) Crosslinked GG-NG		
Surface Roughness	Lower roughness (smoother surface) due to dense, rigid crosslinking.	Higher roughness (uneven surface) from flexible, spacer-like crosslinks.		
Height	Lower height due to less functionalities of GA	Greater height due to more functionalities of MBA.		







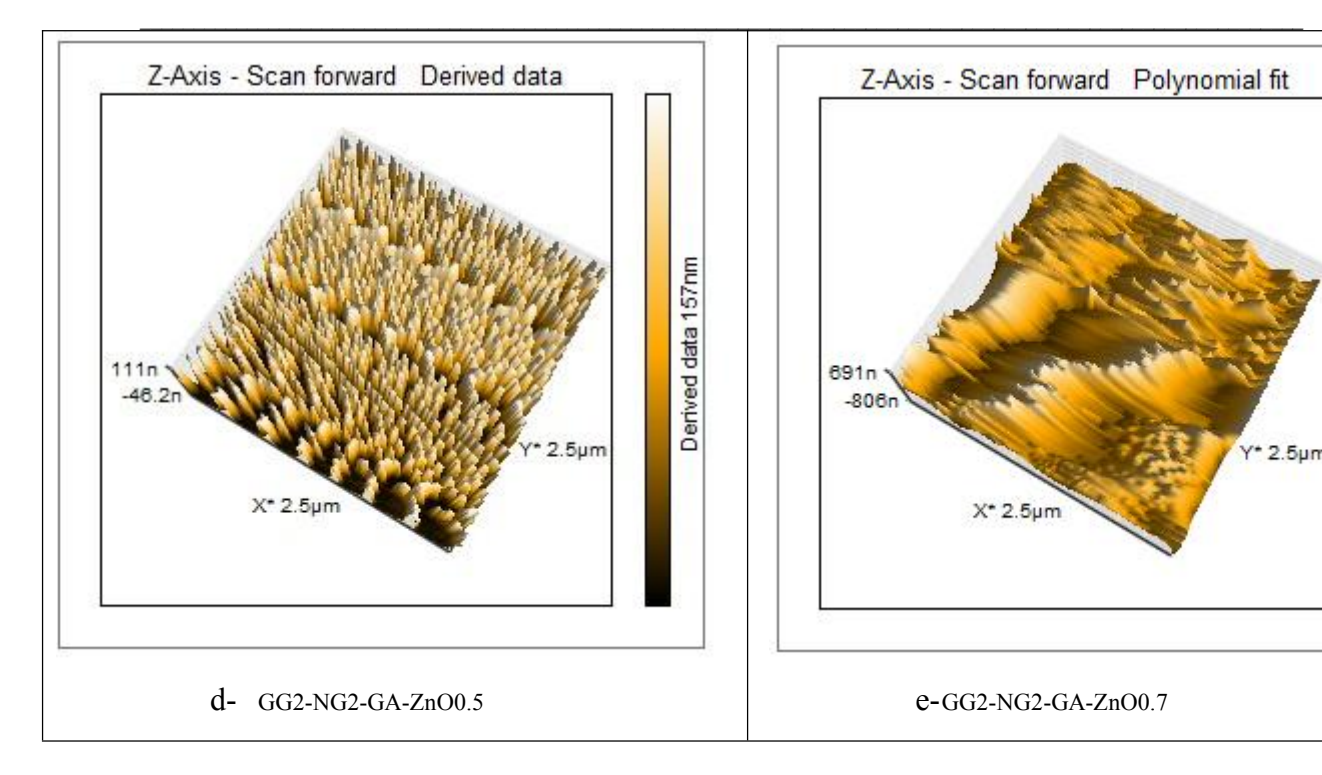


Fig. 4. a- GG2-NG1-GA, b- GG2-NG2-GA, c- GG2-NG1-MBA d- GG2-NG2-GA-ZnO0.5, and e- GG2-NG2-GA-ZnO0.7

Polynomial fit 1.5µm

3.4. SEM features of the prepared biofilms:

The SEM images of GG2-NG1-GA, GG2-NG2-GA, GG2-NG1-MBA, GG2-NG2-GA-ZnO0.5, and GG2-NG2-GA-ZnO0.7 at different views are given in Fig.s 5a-f. The SEM features confirm the AFM data regarding the morphology of the prepared membranes. The surface morphology of GG2-NG1-GA showed a relatively smooth and uniform matrix with some irregularly shaped agglomerates. The clusters appear as bright, dense regions, thus, indicating possible aggregation of components (likely crosslinked regions or residual particulates), Fig. 5a. In addition, small, dispersed granular features can be observed throughout the surface with inconsistent particle size distribution with both fine particles and larger aggregates. The observed indentations and protrusions, possibly indicating uneven crosslinking between the guar gum (GG) and neem gum (NG1). On the other hand, the surface of GG2-NG2-GA was more heterogenous with larger uneven distributed clusters due to increasing the amount of NG in the polymer matrix, Fig. 5b. This assumption is based on polymer fabrication conditions [69]. However, upon investigating the SEM images of GG2-NG1-MBA, Fig.s 5c, d (black and white and colored), one can see that the morphology turned highly porous with relatively uniform voids. This was attributed to the higher functionalities of MBA and the advanced crosslinking power of MBA over GA. reflecting the advanced crosslinking power of MBA with GA regarding its higher functionalities. At last, the SEM images of GG2-NG2-GA-ZnO0.5, and GG2-NG2-GA-ZnO0.7 Fig.s 5e, f show ZnO NPs as shiny scattered masses incorporated within the polymer matrix in random manner which confirms the successful combination between ZnO and polymeric matrices.

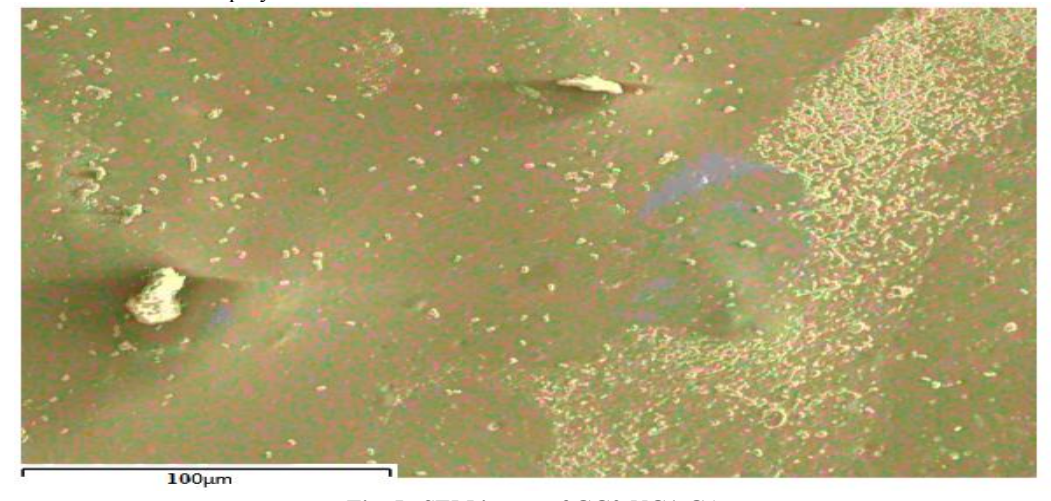


Fig. 5a SEM image of GG2-NG1-GA

Egypt. J. Chem. 69, No. 2 (2026)

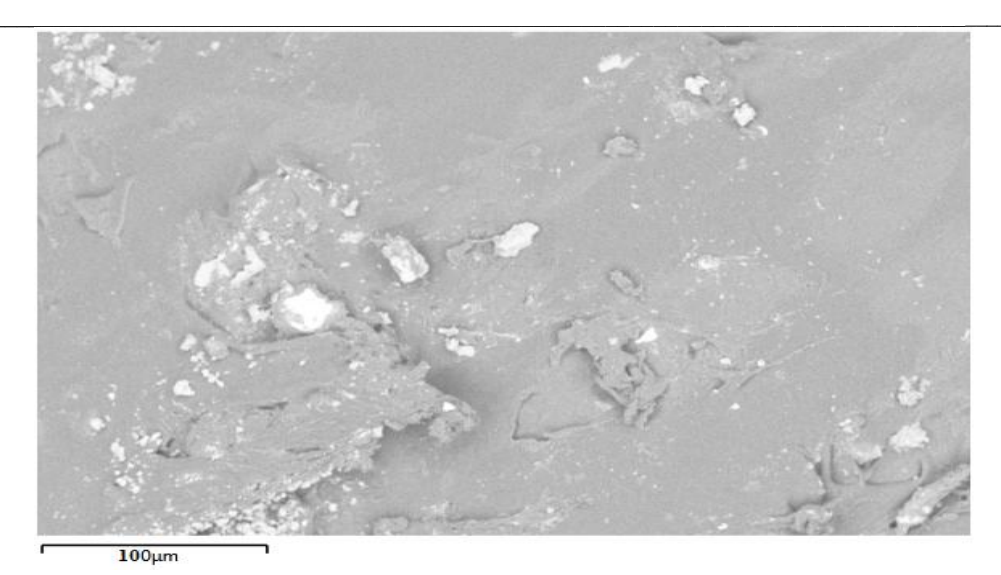
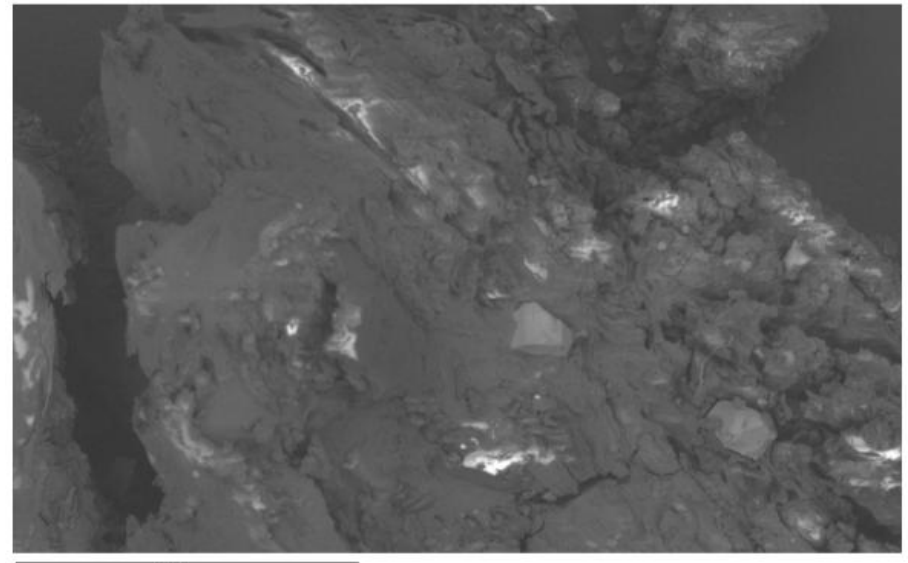


Fig. 5b SEM image of GG2-NG2-GAFig. 5c SEM images of GG2-NG1-MBA



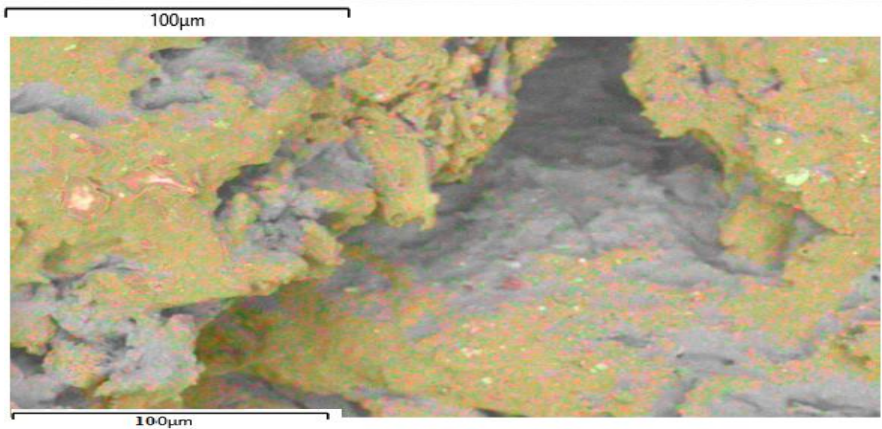


Fig. 5c SEM images of GG2-NG1-MBA

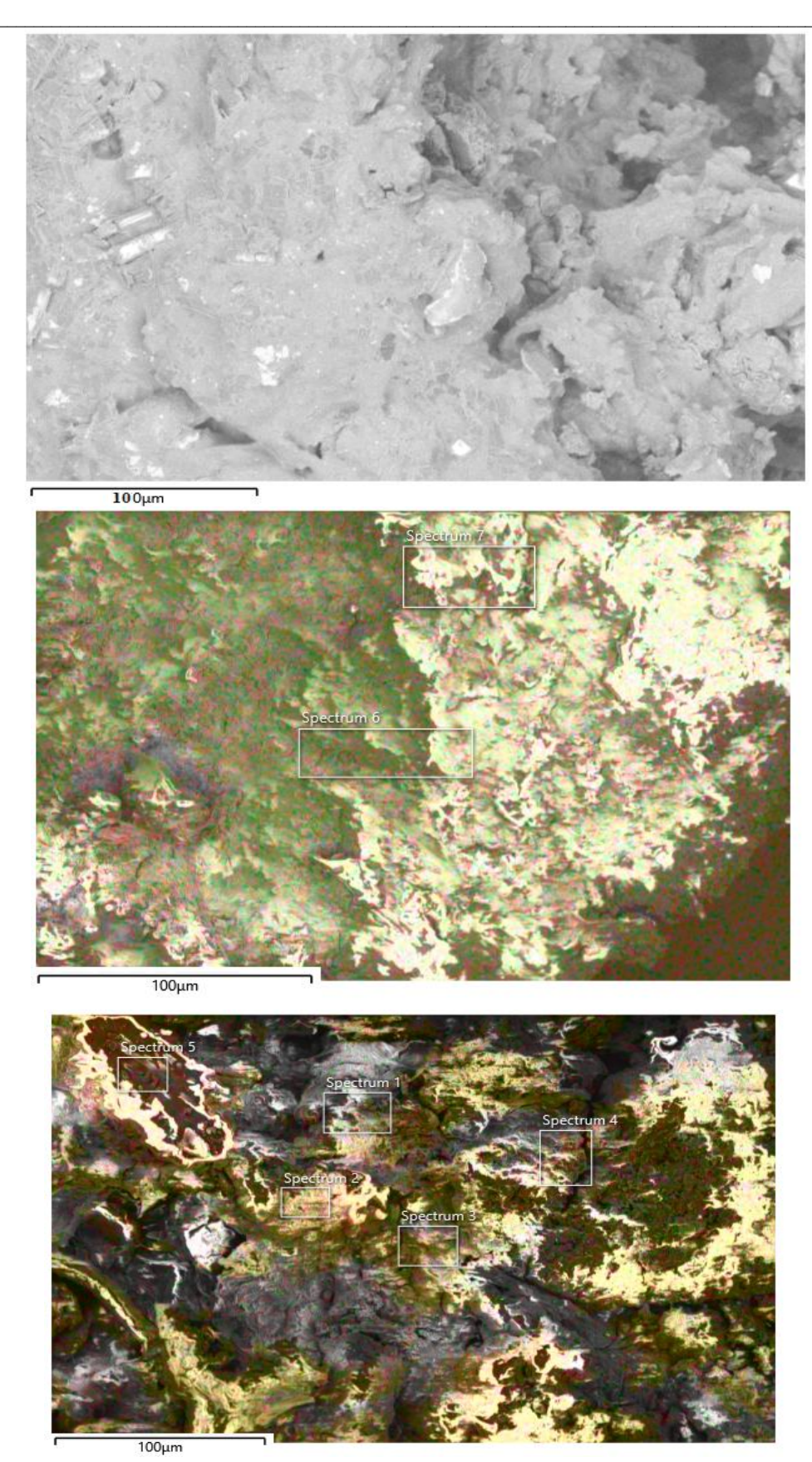


Fig. 5e: The SEM image of GG2-NG2-GA-ZnO0.5

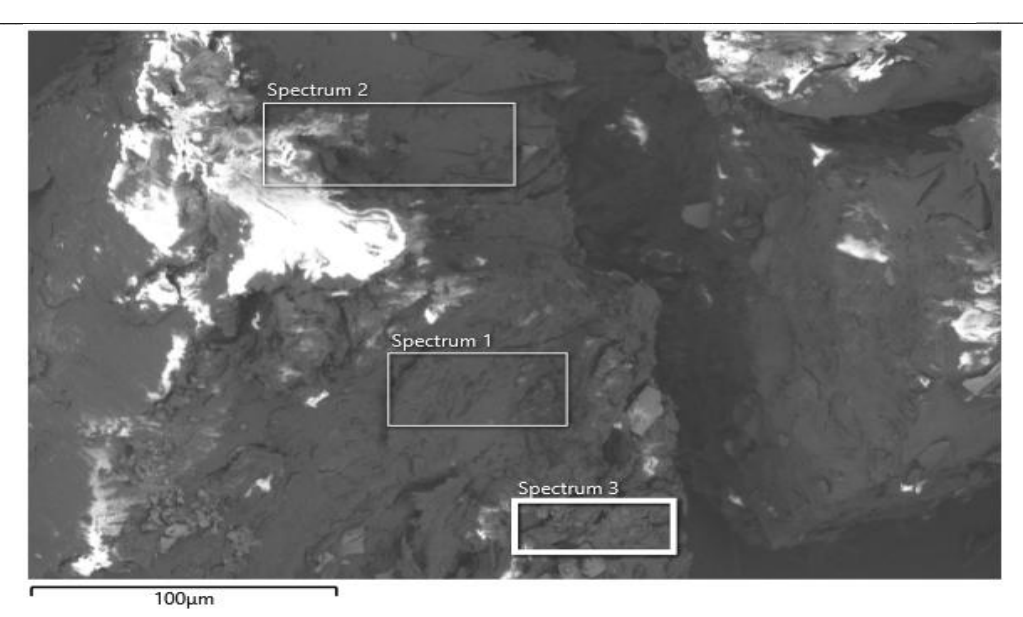
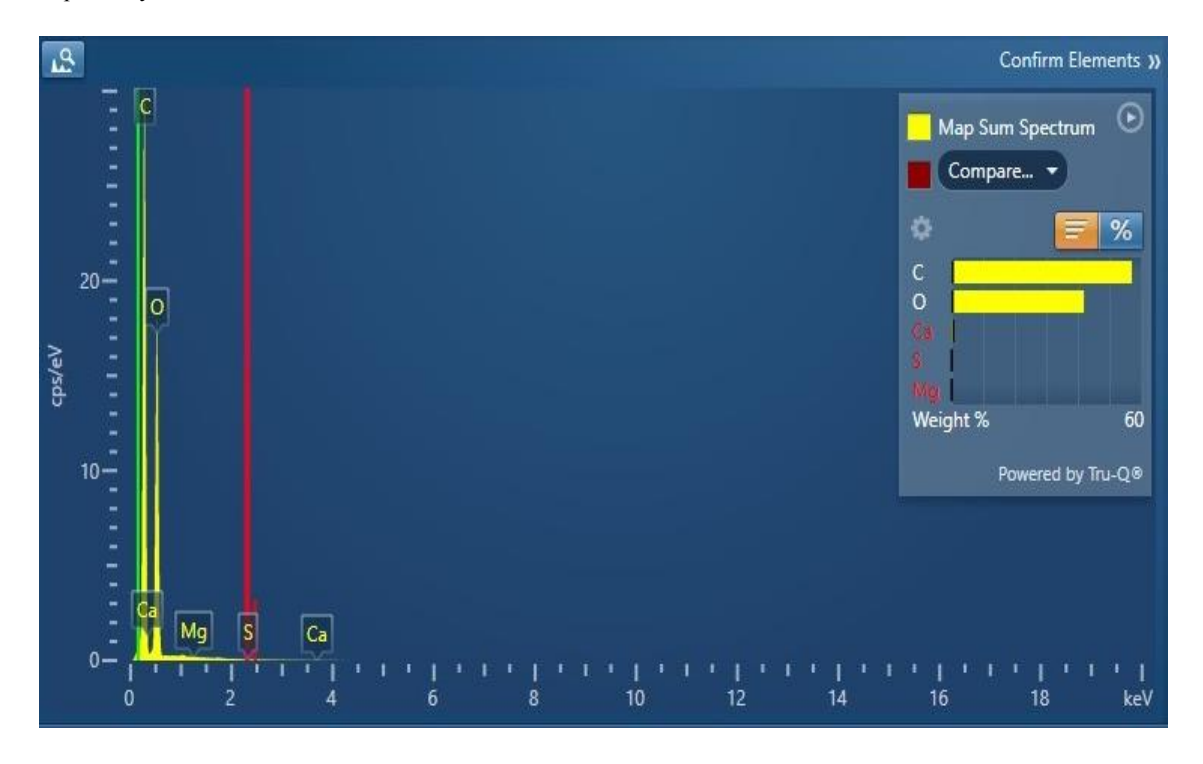


Fig. 5f: The SEM image of GG2-NG2-GA-ZnO0.7
Fig. 5: The SEM images of GG2-NG1-GA, GG2-NG2-GA, GG2-NG1-MBA, GG2-NG2-GA-ZnO0.5, and GG2-NG2-GA-ZnO0.7

3.5. EXD investigation:

EDX mapping and charts of GG2-NG1-GA, GG2-NG2-GA, GG2-NG2-GA-ZnO0.5, and GG2-NG2-GA-ZnO0.7 are given in Fig. 6a-d respectively.



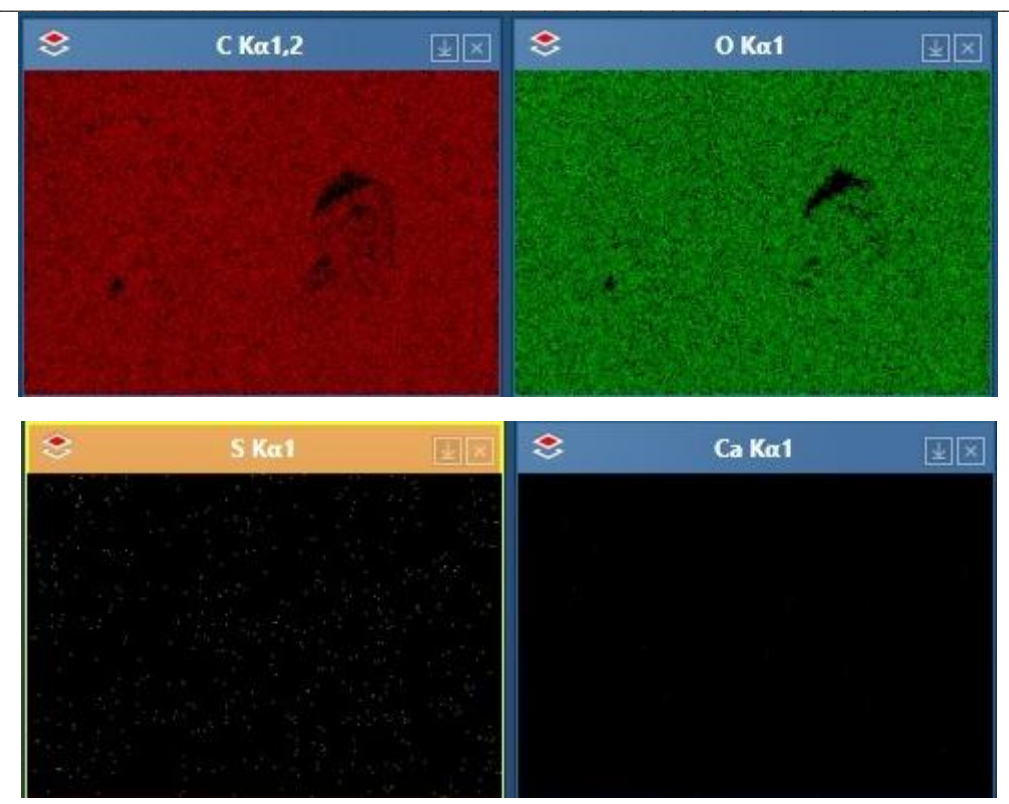


Fig. 6a: EDX mapping of GG2-NG1-GA



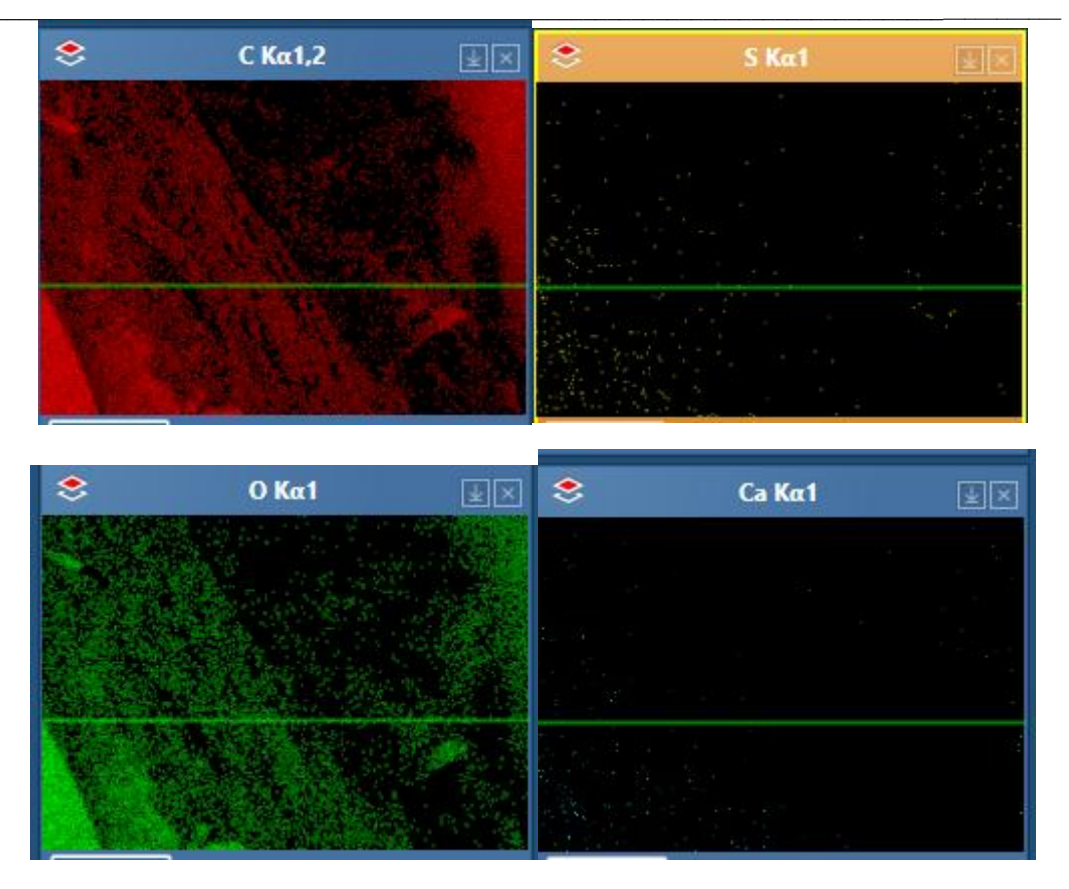
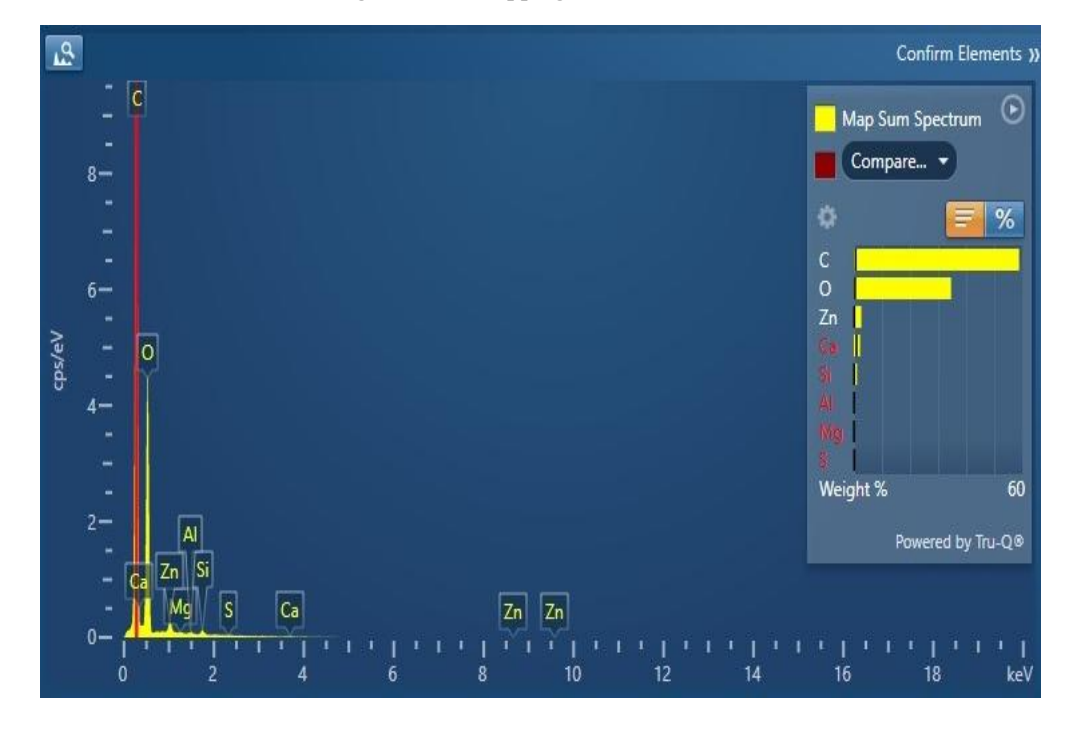


Fig. 6b: EDX mapping of GG2-NG2-GA



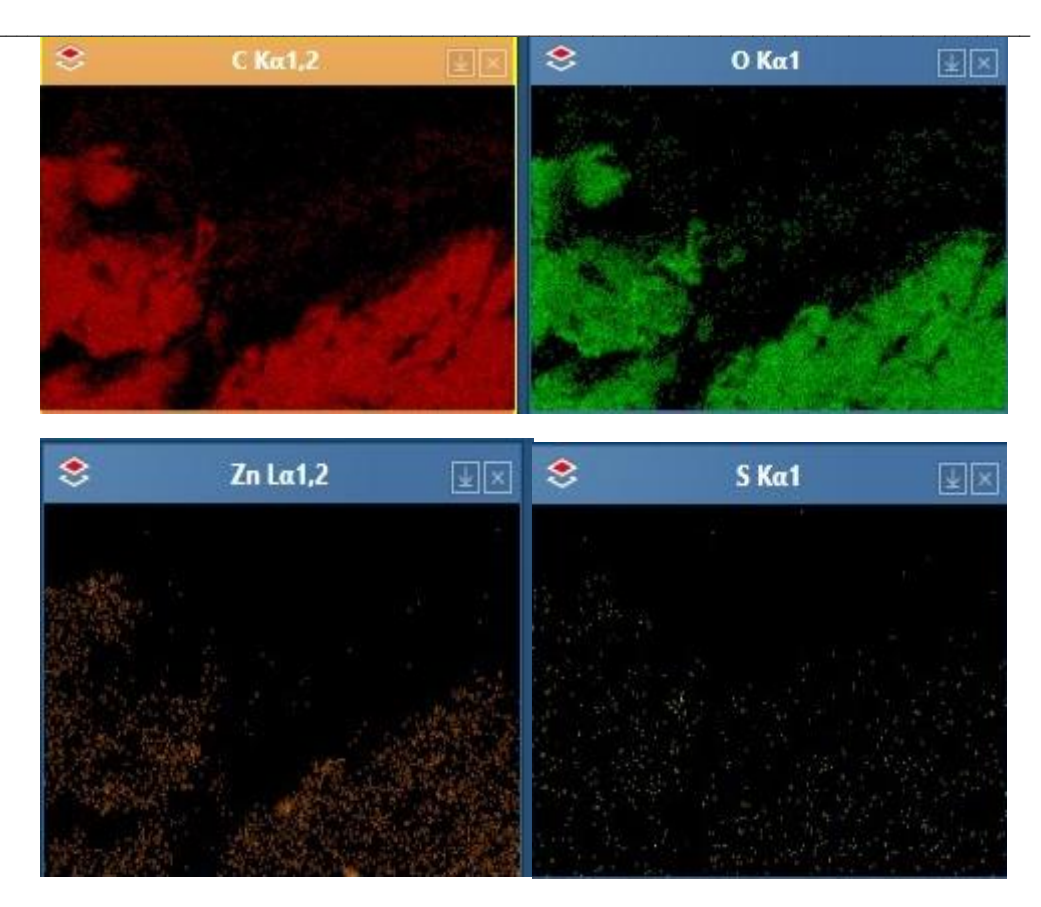
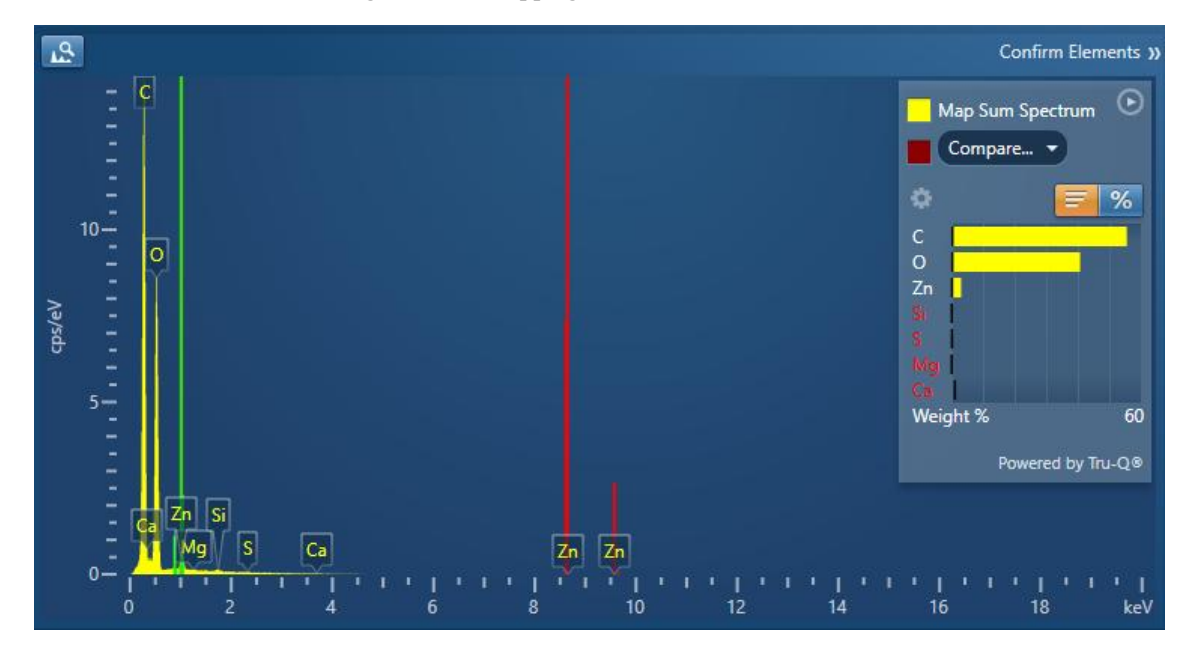


Fig. 6C: EDX mapping of GG2-NG2-GA-ZnO0.5



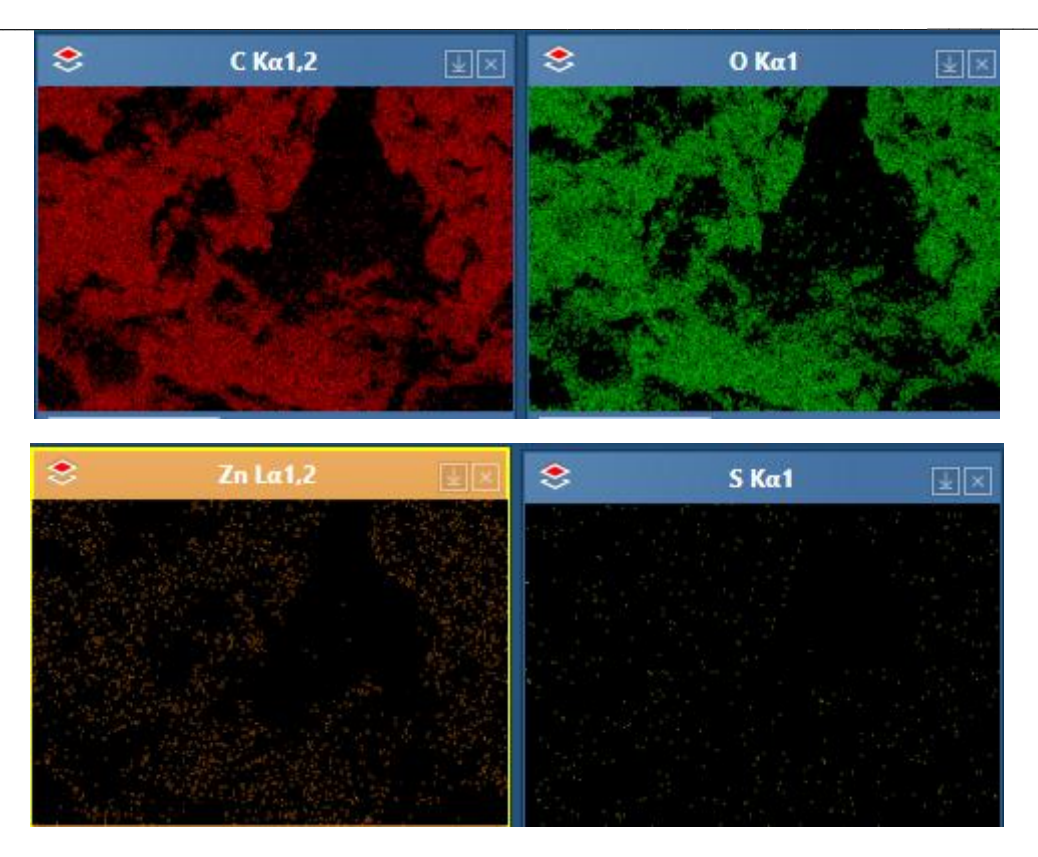


Fig. 6d: EDX mapping of GG2-NG2-GA-ZnO0.7

Fig. 6: EDX mapping of GG2-NG1-GA, GG2-NG2-GA, GG2-NG2-GA-ZnO0.5, and GG2-NG2-GA-ZnO0.7

The bar chart and corresponding spectrum show peaks for the following major elements: Carbon (high peak) indicates a carbon-rich matrix for the major gum units, Oxygen (high peak) which is common for oxygen-based groups that present in gums such as hydroxyl or carbonyl, inorganic elements such as Sulphur, sodium and calcium obtained from natural precursors are also present as traces. Zn is present as minor but observable peaks in GG2-NG2-GA-ZnO0.5 and strong dominant peaks in GG2-NG2-GA-ZnO0.7. Thus, the overall EDX analyses confirm that the membranes are majorly carbonaceous composites with dominant carbon and oxygen, and minor elements while zinc predominates in zinc containing biofilms approving successful incorporation.

3.6. Antimicrobial activity of the prepared membranes:

The biofilms are comprised of GG which is a natural polysaccharide with film-forming ability but limited inherent antimicrobial activity, NG with proved mild antimicrobial properties, GA as a potent biocidal crosslinker, MBA which is a synthetic crosslinker with less antimicrobial and ZnO NPs which are known for potential broad-spectrum antimicrobial activity. The antimicrobial activity is given in Fig. 7 and the inhibition zones are given in Table 4.

The antimicrobial activity of the biofilms was evaluated against different pathogens including Bacillus subtilis and Staphylococcus aureus as Gram positive bacteria, Klebsiella pneumoniae and Escherichia coli as Gram-negative bacteria and Candida Albican and Aspergillus niger as infective fungi.

The preliminary antimicrobial activity was determined using agar method [70], and the results were documented for each tested product as average diameter of the inhibitory zones (d) of fungal or bacterial growth surrounding the disks at a concentration of 100 mg/mL in dimethyl sulfoxide.

The provided data revealed that most of the synthesized composites exhibited varying degrees of inhibition against the tested microorganisms in comparison with standard drugs.

Basically, it was noticed that GG2-NG2-GA-ZnO0.7 demonstrated the potent antibacterial activity against Bacillus subtilis and Candida albicans with average diameters of the inhibitory zones 24.6 and 21.9 mm. This may be attributed to the synergistic action of ZnO and NG. On the other hand, all the tested samples showed lower to no activity against Aspergillus

niger in spite of their observed high activity against Candida albicans. All the prepared biofilms showed comparable antimicrobial activity with respect to the control antibiotic. This finding is in an accordance with the previous results reported by many researchers [71–73].

The net antimicrobial data are as following:

GG2-NG2-GA-ZnO0.7: Most consistent and highest activity across both Gram-positive and fungal strains due to the synergistic antimicrobial effects of ZnO and neem gum specially against Gram-positive bacteria and fungi.

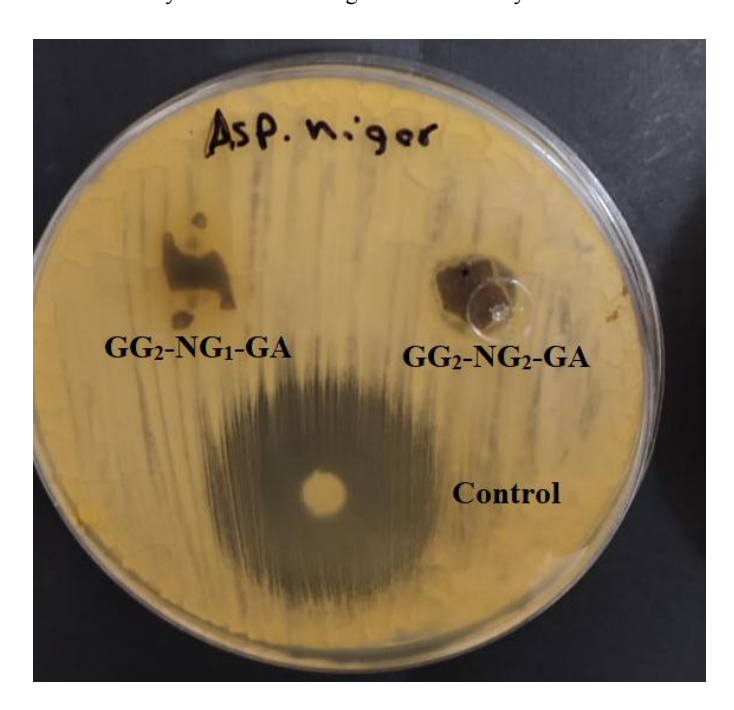
GG2-NG2-GA and GG2-NG1-GA displayed strong to moderate activity due to GA's strong biocidal properties but lack of ZnO reduced effectiveness slightly.

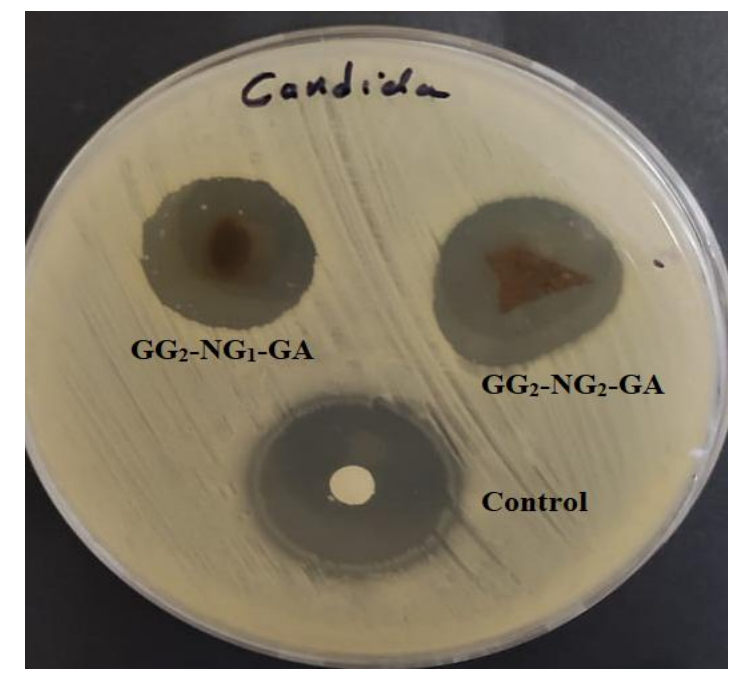
GG2-NG1-MBA: Least effective of the active formulations. MBA contributed no direct antimicrobial action, only structural support. On the other hand, noticeable resistance of Aspergillus niger indicates the need for stronger antifungal components for broad-spectrum protection. This result aligns with prior studies showing that A. niger's robust cell wall and enzymatic detoxification mechanisms often confer resistance to natural antimicrobials like neem extracts (Wylie MR, Merrell DS. The Antimicrobial Potential of the Neem Tree Azadirachta indica. Front Pharmacol. 2022 May 30;13:891535. doi: 10.3389/fphar.2022.891535. PMID: 35712721; PMCID: PMC9195866.). To enhance antifungal performance, we propose the following modifications for future work:

Synergistic Additives: Incorporating low doses of antifungal agents (e.g., chitosan, essential oils like clove or thyme) could exploit multi-target mechanisms to overcome A. niger's resistance.

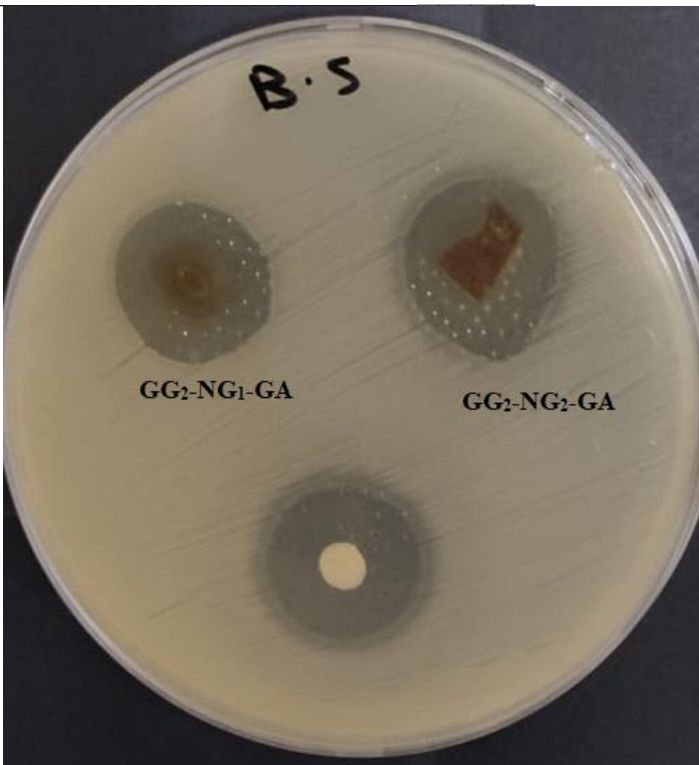
ZnO Nanoparticle Functionalization: Increasing ZnO concentration (beyond the 0.7% tested here) or reducing particle size may improve fungal inhibition, as ZnO disrupts cell membranes and ROS generation.

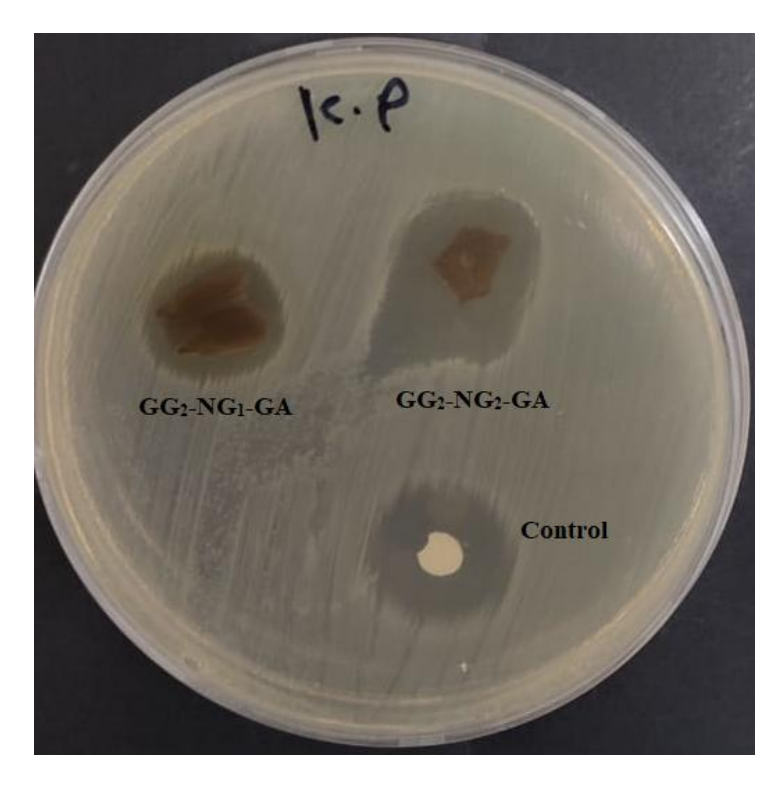
Crosslinker Optimization: Switching to crosslinkers with inherent antifungal properties (e.g., citric acid) could augment activity while maintaining material stability.

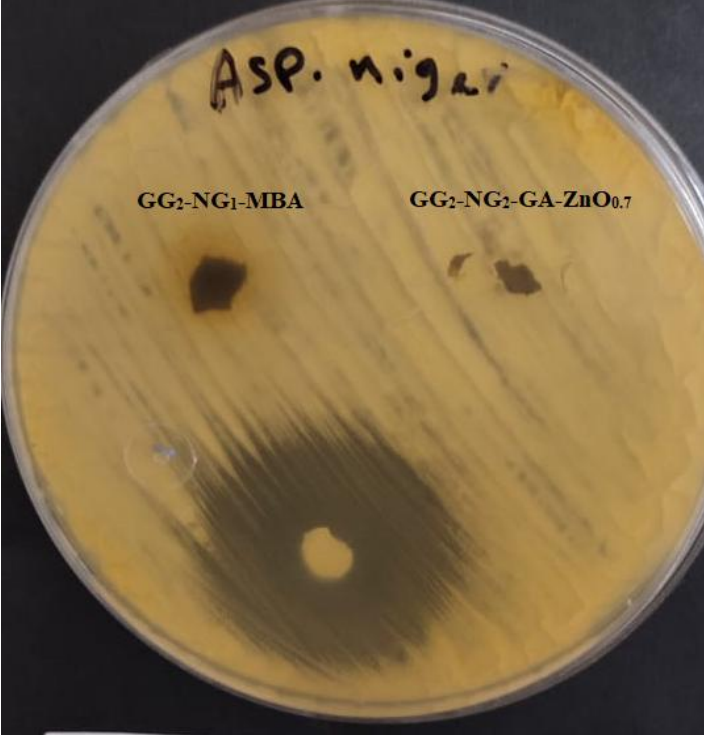




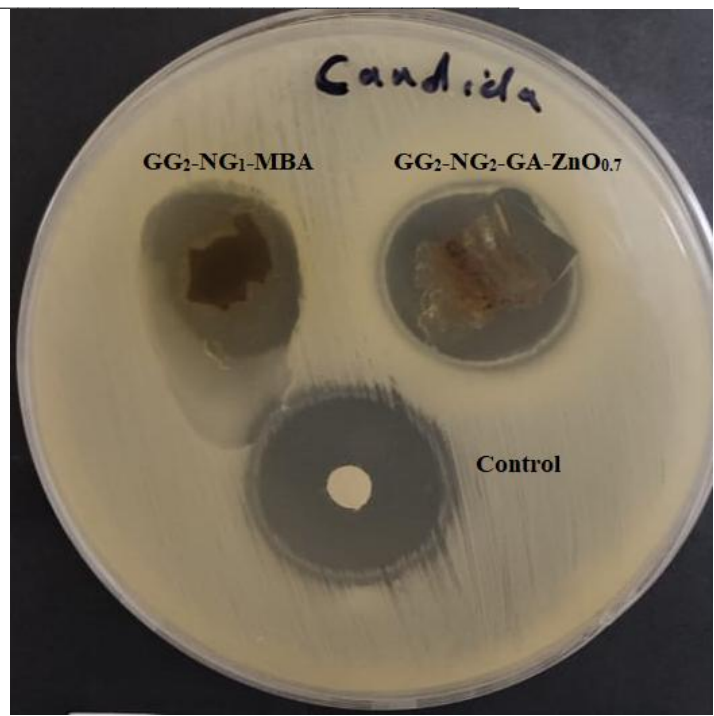


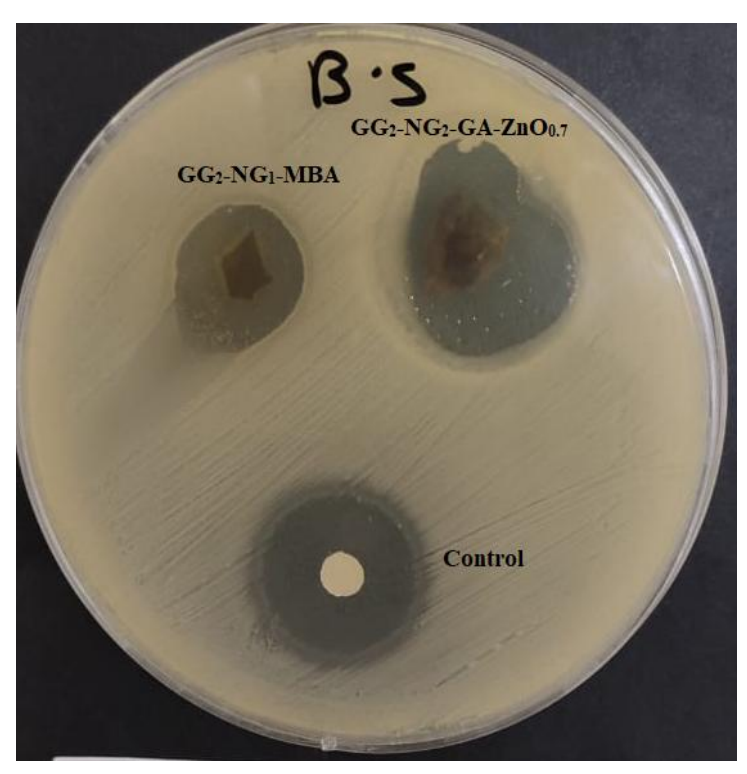














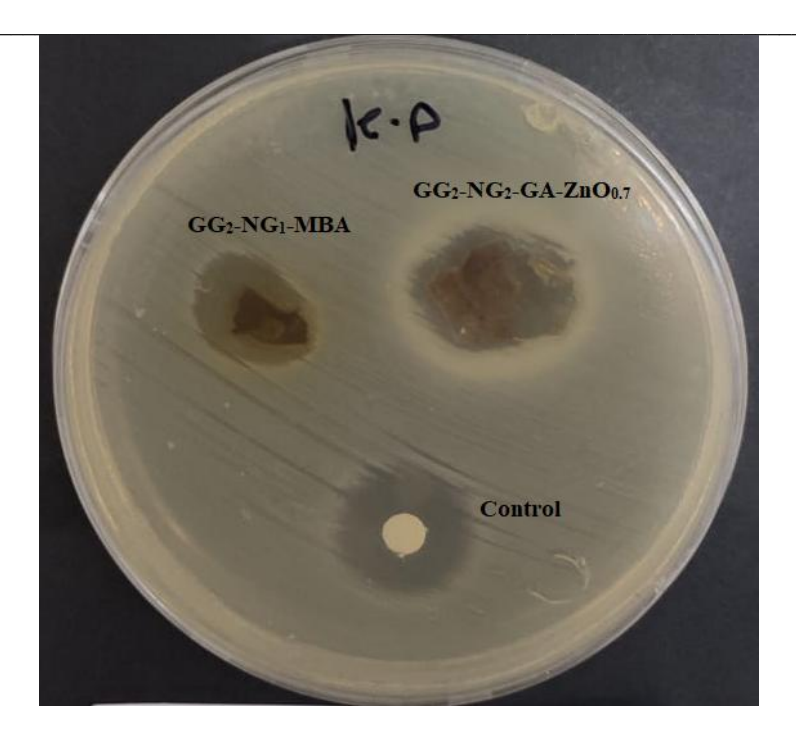


Fig. 7: Antimicrobial Activity of the prepared biofilms

Table 4: Inhibition zones of the investigated biofilms towards various Gram-positive, Gram-negative bacteria and some fungal species

Microorganism	GG2-NG1- GA	GG2-NG2- GA	GG2-NG1- MBA	GG2-NG2-GA- ZnO0.7	Control Antibiotic
Bacillus subtilis (ATCC 6633)	18 ± 2	23 ± 1	12.7 ± 0.5	24.6 ± 0.5	21 ± 0.1
Staph. aureus (ATCC 6538)	15 ± 2	NA	18.5 ± 0.5	16.4 ± 0.5	19 ± 0.2
Escherichia coli (ATCC 8739)	20 ± 1	16 ± 1	9.4 ± 0.5	10.7 ± 0.5	16 ± 0.1
Klebsiella pneumoniae (ATCC 13883)	15 ± 2	16 ± 1	13.3 ± 0.5	14.6 ± 0.5	20 ± 0.1
Candida albicans (ATCC 10221)	22 ± 2	20 ± 2	19.7 ± 0.5	21.9 ± 0.5	25 ± 0.2
Aspergillus niger (ATCC 16888)	NA	NA	NA	NA	34 ± 0.1

^{*} NA: No activity

3.7. Investigating the physical properties of the biofilms

3.7.1. Solubility:

Water solubility is a critical parameter in evaluating membranes for packaging materials, as it directly influences their functionality and environmental impact [74]. Highly soluble films are advantageous for applications requiring biodegradability, such as single-use edible packaging or dissolvable wrappers, where rapid disintegration is desired [75]. On the other hand, low water solubility is essential for moisture-resistant packaging to protect contents in humid conditions [76]. Balancing solubility ensures optimal performance, shelf-life stability, and compliance with sustainability goals. Therefore, understanding and tailoring water solubility is vital for designing advanced packaging materials that meet both practical and ecological demands [76]. Water solubility of the investigated membranes is presented in Fig. [8]. It can be observed that the order of water solubility is as following: GG2-NG1-GA > GG2-NG2-GA > GG2-NG1-MBA > GG2-NG2-GA-ZnO0.5 > GG2-NG2-GA-ZnO0.7. This finding is based on structural composition considering GA-crosslinked films are more soluble than MBA-crosslinked ones due to MBA's hydrophobic backbone. Increasing NG content slightly reduces solubility (NG2 < NG1). ZnO nanoparticles significantly decrease solubility in a dose-dependent manner (higher ZnO = lower solubility).

^{*} Control for Bacteria was Gentamycin and for fungi was fluconazole at concentration 1.0 mg/ml.

^{* 50} mg of the samples were dissolved in 1.0 mL DMSO

3.7.2. Water vapor permeability (WVP):

Water vapor permeability (WVP) is a key factor in defining the effectiveness of packaging materials, as it directs moisture exchange between the product and its environment. Low WVP is essential for preserving moisture-sensitive goods (e.g., dry foods, pharmaceuticals), preventing spoilage and extending shelf life. Conversely, controlled WVP is needed for fresh products packs to avoid condensation and microbial growth [77]. Thus, the barrier performance must balance protection with biodegradability, especially in sustainable materials. Therefore, optimizing WVP ensures functionality, product stability, and compliance with industry and environmental standards [78]. The water vapor permeability (WVP) of the biofilms are highly influenced by their composition, particularly crosslinking density, hydrophilicity, and nanoparticle incorporation [78]. WVP of the prepared biofilms are given in Fig. 8. It is clear that the trend runs in the order: GG2-NG1-GA > GG2-NG2-GA > GG2-NG2-GA-ZnO0.5 > GG2-NG2-GA-ZnO0.7. This trend is controlled by several key factors. At first, the increase in the hydrophilic components (GG and NG) caused an increase in WVP due to high affinity for water vapor absorption and diffusion [79]. Then, MBA is more hydrophobic than GA and it hindered water vapor diffusion [79]. At last, ZnO NPs further decreased WVP by creating tortuous pathways for vapor diffusion and adding hydrophobic barriers [78]. This trend aligned with typical biopolymer film behavior, where barrier properties improve with reduced free volume and increased hydrophobicity.

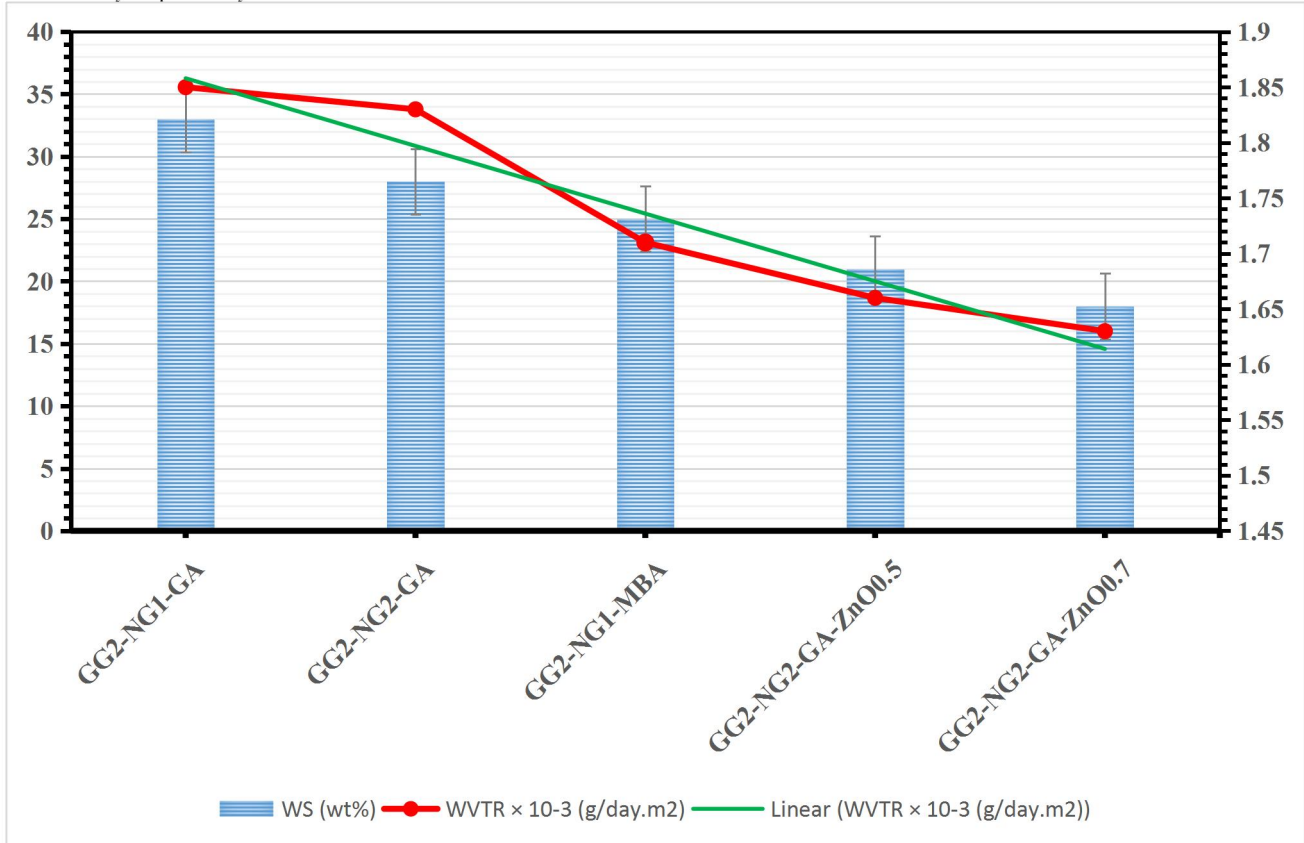


Fig. 8: WS and WVTR of the prepared biofilms

3.7.3. Water Holding capacity (WHC)

Water Holding Capacity (WHC) is a crucial parameter in evaluating the suitability of biopolymer-based membranes, especially when they are intended for packaging applications. Hence, WHC measures the ability of a membrane to absorb and retain water without disintegration. Usually, it is an indicator of the hydrophilic nature and swelling behavior of the membrane. In packaging application, high WHC indicates the film can absorb moisture without losing structural integrity, making it suitable for food packaging where moisture management is essential. WHC of the prepared membranes is given in Fig. 9. It can be seen that GG2-NG1-GA displayed the highest WHC due to its high content of GG which is naturally hydrophilic. On the other hand, upon doubling the NG content (GG2-NG2-GA), the WHC value decreased from 67% to 40% only. Further reduction was observed when replacing GA was replaced by the stronger crosslinking agent MBA. Thus, the observed WHC for sample (GG2-NG1-MBA) was only 27%, implying a more compact structure with lower hydrophilicity. On the other hand, the effect of imbedding moderate amount of ZnO NPs shows balanced WHC which was reduced at higher ZnO NPs concentration. (50% for GG2-NG2-GA-ZnO0.5 and 23% for GG2-NG2-GA-ZnO0.7, respectively) due to the hydrophobic nature of ZnO NPs [80]. Generally, among the GG-NG membranes, GG2-NG1-GA showed the highest WHC due to the hydrophilic nature of GG and moderate crosslinking.

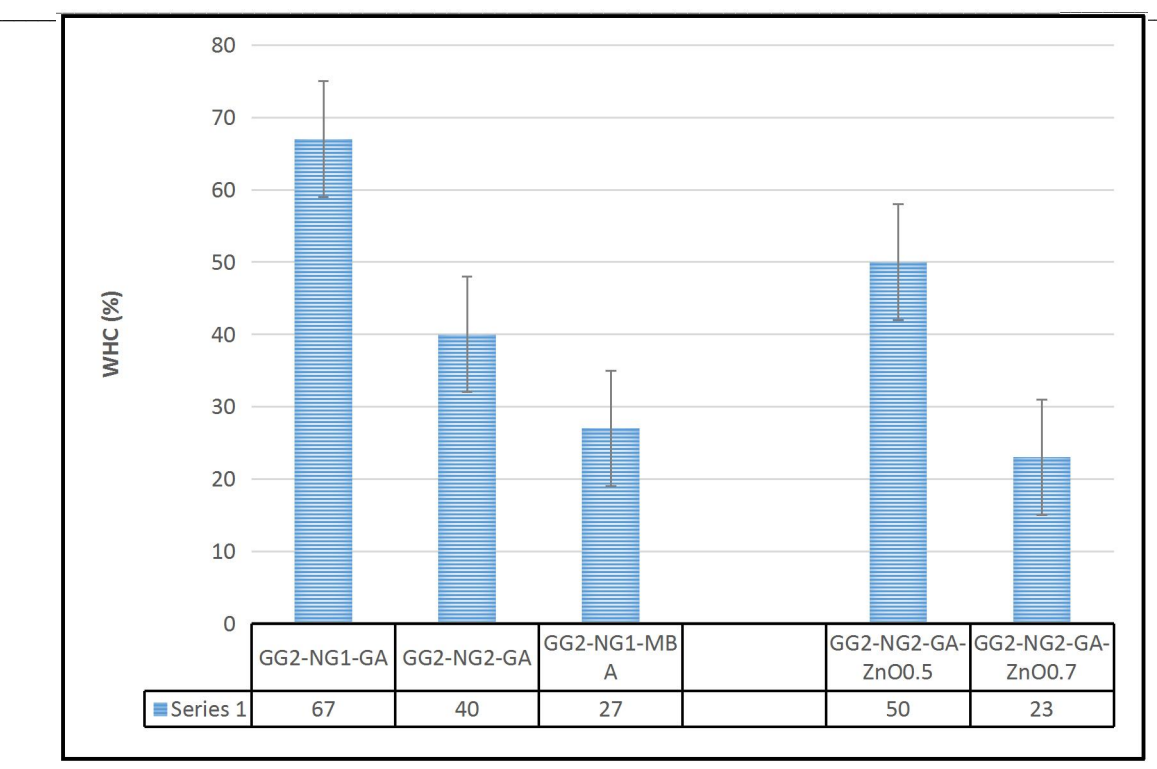


Fig. 9: WHC of the prepared GG-NG membranes

3.8. Surface hydrophobicity (Contact angle)

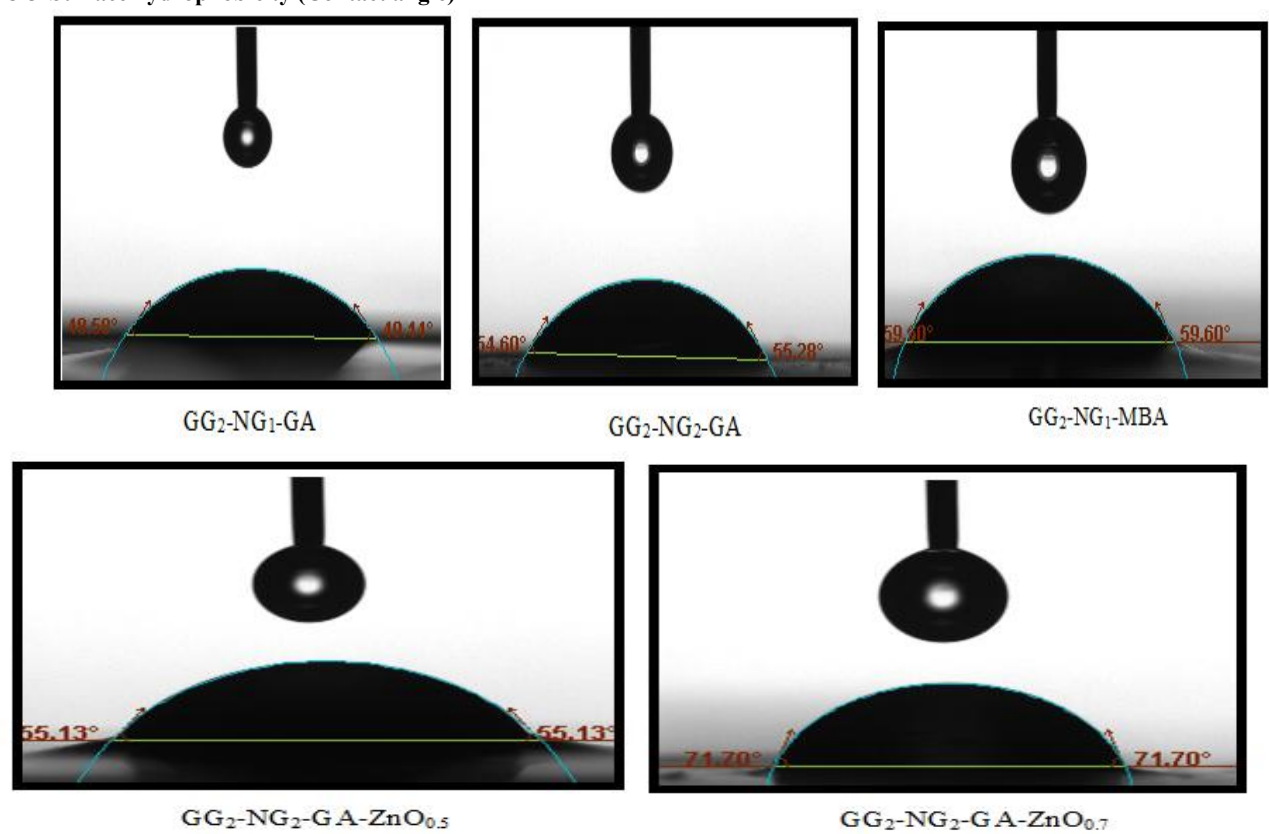


Fig. 10: Contact angles of the prepared membranes

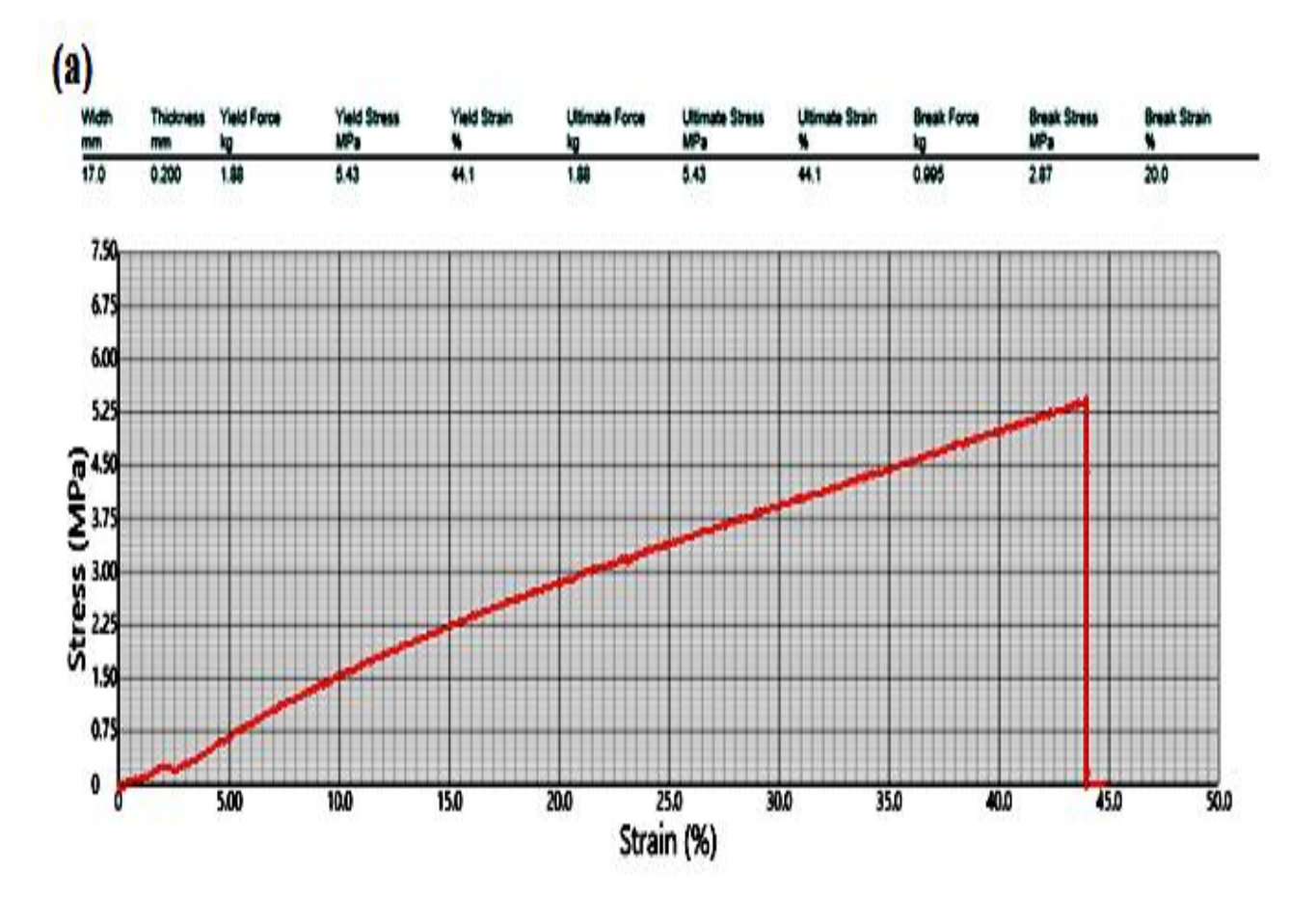
Egypt. J. Chem. **69**, No. 2 (2026)

Measuring the contact angle of prepared biofilms is important to reveal valuable information about their surface properties and wettability. The contact angle helps to predict how liquids will spread on the surface, which is particularly relevant for packaging materials as it directly affects the quality and shelf life of the packed products. The wettability (hydrophilic/hydrophobic) properties of guar gum/neem gum- based membranes were evaluated by measuring the water contact angles as shown in Fig. 10. The contact angle value of GG2-NG1-GA film was found to be 49.44°, whereas it was 55.28° for GG2-NG2-GA indicated that neem gum increased the hydrophobicity of the biofilm. It is interesting to mention that after incorporating methylene bisacrylamide (GG2-NG1-GA film), contact angle increased to 59.6° due to the compactness of the film components after crosslinking by MBA. Similarly, Rahman and their colleagues has also stated that after crosslinking contact angle of films increased [81]. The highest contact angle was observed for GG2-NG2-GA-ZnO0.7 due to incorporation of ZnO NPs as reinforcing material [82,83].

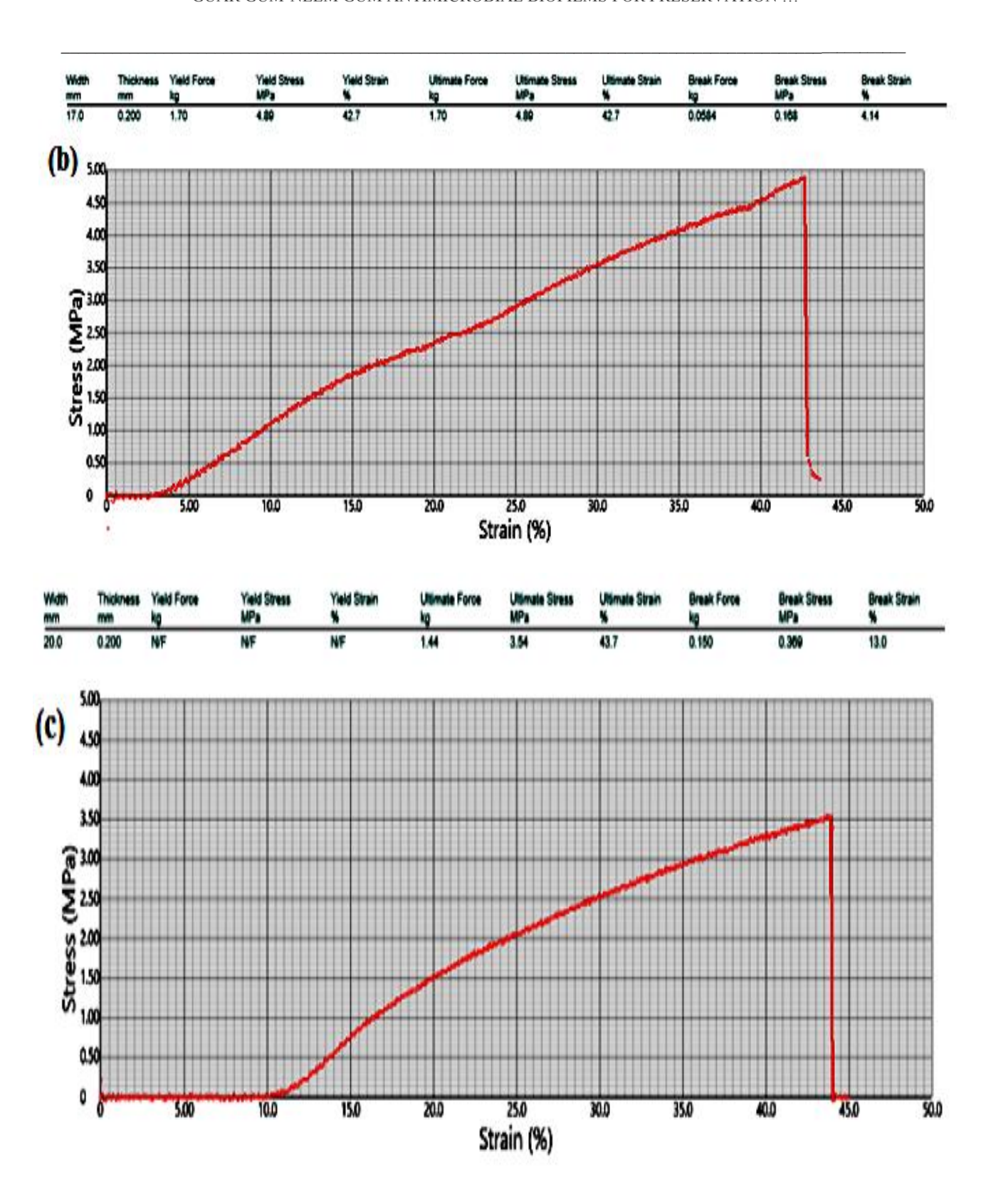
3.9. Mechanical properties of the prepared biofilms:

Stress-strain curves of GG2-NG1-GA, GG2-NG2-GA, GG2-NG1-MBA GG2-NG2-GA-ZnO0.5, and GG2-NG2-GA-ZnO0.7 are given in Fig. 11. The results highlight structural variations in stress and elongation percentages across different samples. The samples are classified into two groups:

- 1. Group 1: GA Crosslinked (without ZnO)
 - o GG2-NG1-GA (flexible, lower stiffness)
 - GG2-NG2-GA (slightly stiffer, more elongation)
 - o GG2-NG1-MBA (more rigid, lower elongation)
- 2. Group 2: GA Crosslinked (with ZnO)
 - o GG2-NG2-GA-ZnO0.5 (moderate stiffness, higher than GA alone)
 - o GG2-NG2-GA-ZnO0.7 (highest stiffness, reduced elongation)



Egypt. J. Chem. 69, No. 2 (2026)



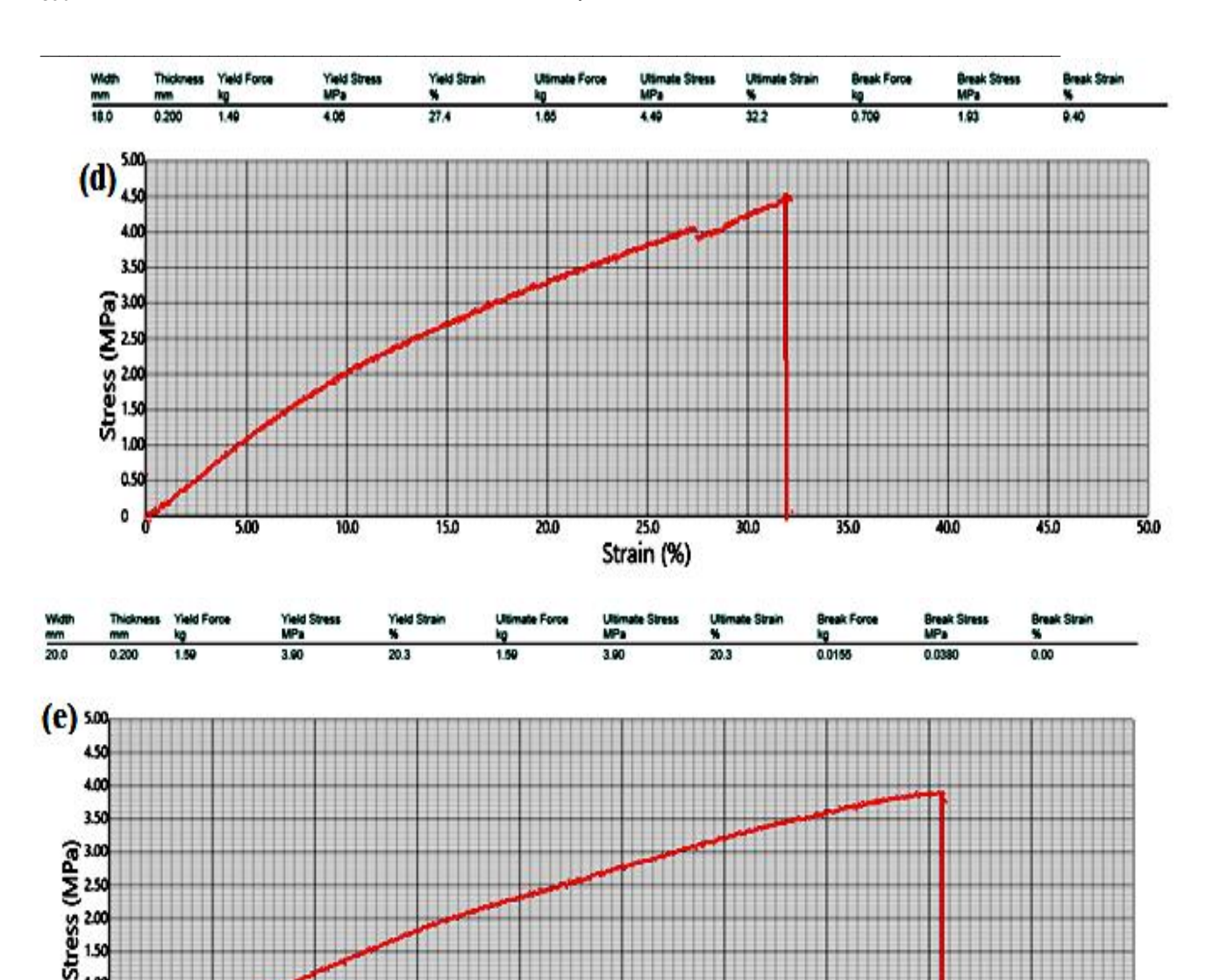


Fig. 11: Stress-strain curves of the prepared membranes (a- GG2-NG1-GA, b- GG2-NG2-GA, c- GG2-NG1-MBA, d-GG2-NG2-GA-ZnO0.5, and e- GG2-NG2-GA-ZnO0.7)

Strain (%)

17.5

22.5

10.0

3.10. Mechanical Properties in relevance to SEM Images:

5.00

The mechanical properties of the prepared biofilms were correlated to the data extracted from their SEM images. It can be seen that the surface of GG2-NG1-GA (Fig. 5a) shows a relatively smooth matrix with some irregularly shaped aggregates and clusters. This implies good film formation and cohesion, which can be translated to accordingly, adequate tensile strength. However, the presence of clusters suggests potential weak points, which may reduce the overall strength under stress and can lead to heterogenous mechanical behavior and stress concentration concentrated points [84]. Therefore, the balance between of smooth and clustered regions indicates that GG2-NG1-GA may exhibit moderate tensile strength and good flexibility. On the other hand, the SEM image of GG2-NG2-GA (Fig. 5b) shows a rough and uneven surface with large aggregates and irregular particles scattered throughout. In addition, and the matrix appears densely packed with some crystalline-like structures protruding from the surface. Also, there are deep grooves and cracks, indicating poor film continuity [85]. Consequently, the film exhibits high stiffness and low flexibility, thus, making it is less suitable for packaging applications where ductility and toughness are essential. In comparison, the SEM image of GG2-NG1-MBA (Fig. 5c) shows a highly porous and cracked structure with significant roughness indicating poor film cohesion. Such a structure indicates low tensile strength and poor mechanical integrity due to the presence of microvoids and cracks. Also, the highly porous nature can lead

to increased water absorption, with the subsequent reduction of film stability in humid conditions. Thus, the application of MBA as a crosslinker increased tensile strength and reduced elasticity [86]. Considering the relevance between the SEM features of GG2-NG2-GA-ZnO0.5 (Fig. 5e) and its mechanical properties, the image shows a rough, granular surface with embedded particulate structures with where some areas exhibit crystalline-like features, likely indicating the presence of ZnO nanoparticles. The matrix appears dense and compact, but with some protruding particles. Thus, the addition of ZnO nanoparticles has resulted in heterogeneous distribution, which can act as reinforcement sites. However, the rough texture indicates that the nanoparticles are not uniformly embedded, which might affect the mechanical homogeneity. Nevertheless, despite the roughness, the film appears denser and less porous compared to the previous GG2-NG2-GA sample. In brief, embedding ZnO NPs tends to increase the stiffness of the polymer matrix due to their rigid, crystalline nature and to improve compactness [87,88], indicating good interaction between the crosslinked GG-NG matrix and ZnO. Overall, it worth mentioning that the films incorporating ZnO NPs showed poor strength compared to non-reinforced samples due to that the stiff crystalline regions might reduce the elongation, thus, making the films less flexible. Therefore, proper interfacial bonding between ZnO and the polymer is crucial for maintaining mechanical integrity. Yet, the inconsistent distribution of ZnO particles caused localized stiffness, leading to uneven stress distribution under load. The film appears relatively uniform compared to previous samples, indicating better film formation and matrix stabilization aided by embedded ZnO NPs [89]. In conclusion: the aforementioned observations can be summarized as follows:

- O Group 1: Increasing neem gum (NG2 vs. NG1) resulted in higher elongation, but MBA crosslinking lead to relatively higher stiffness and lower elongation.
- Group 2: Increasing ZnO content (0.5 to 0.7) results in increased stiffness and slightly reduced elongation.

Future Perspectives of Biofilms for Preserving Biological Samples Using Guar Gum/Neem Gum Membranes. Biofilms composed of guar gum and neem gum hold promising potential for the preservation of biological samples due to their biocompatibility, antimicrobial properties, and eco-friendly nature. Future research could focus on optimizing their mechanical strength and barrier efficiency to enhance long-term sample stability. Incorporating active components in nanoform may further improve their antibacterial and antifungal performance. Scalable production methods, such as electrospinning or 3D printing, could make these membranes more accessible for medical and industrial applications. Additionally, their biodegradability aligns with sustainable practices, reducing environmental impact compared to synthetic alternatives. Clinical trials may explore their efficacy in preserving tissues, vaccines, or microbial cultures under varying conditions. Ultimately, these natural polymer-based biofilms could revolutionize bio-preservation by offering cost-effective, non-toxic, and highly functional solutions.

4. Conclusions:

In this work, five crosslinked guar gum-neem gum (GG-NG) biofilms were successfully prepared via thermal crosslinking using two crosslinkers (glutaraldehyde, GA, and N,N'-methylenebisacrylamide, MBA), with ZnO nanoparticles incorporated in selected formulations to reinforce the films and enhance their antimicrobial activity. The prepared biofilms were comprehensively characterized by FTIR, AFM, SEM, and other analytical tools. FTIR analysis confirmed successful crosslinking and embedding of ZnO by showing characteristic peak shifts, broadening, and overlap. The designed structural variations significantly influenced the physicochemical properties of the biofilms. AFM and SEM images revealed topographical differences depending on the crosslinker type, GG/NG ratio, and ZnO content.

The water holding capacity (WHC) and water solubility (WS) of the membranes followed the order: GG2-NG1-GA > GG2-NG2-GA > GG2-NG1-MBA > GG2-NG2-GA-ZnO0.5 > GG2-NG2-GA-ZnO0.7. Among all, the GG_2 -NG₁ -GA sample demonstrated the most promising overall properties:

- Strength: Moderate (5 MPa), adequate for packaging and preservation without being overly rigid.
- Flexibility: High stretchability and good ductility.
- Durability: Balanced strength and flexibility.
- Cost-effectiveness: Utilizes GA as a more economical crosslinker.
- Biodegradability: Composed mainly of natural gums with minimal synthetic additives.

Key findings include:

- 1. The inclusion of ZnO nanoparticles increases rigidity and reduces elasticity.
- 2. Crosslinkers (GA and MBA) enhance tensile strength, with MBA being slightly more effective.
- 3. Higher ZnO content (0.7%) causes brittleness and lowest ductility.
- The GG2-NG1-GA formulation achieves the best balance between mechanical strength, flexibility, and ecofriendliness.

Declaration statements:

Ethical Approval

Ethical approval is not applicable for this article.

Consent to Participate

The authors confirm that all data included in this study are original experimental data and outcomes.

Consent to Publish

The authors give their permission for the publication of recognizable details to be published in the above Journal.

Funding

No funding was received for the present work.

Competing Interests

The authors declare no conflict of interest.

Availability of data and materials

The data that support the findings of this study are all accessible in the present work.

Authors Contributions

Ahmed E. Elhassany: Experimental and data curation, Iman A. Gadelkarim: Supervision, and review, Mohamed S. Behalo: Supervision, data curation, review. Manar El-Sayed Abdel-Raouf: Supervision, Investigation, Validation, Methodology, Formal analysis, Writing - original draft, Writing - review& editing, Mohamed Keshawy: Experimental and reference citation.

Declaration of competing interest

The authors declare that they have no known competing financial interests or personal relationships that could have appeared to influence the work reported in this paper.

5. References and Bibliography

- [1] K.B.N. De Silva, K.S. Dharmasiri, M.P.A.A. Buddhadasa, K.G.N.U. Ranaweera, CRIMINAL INVESTIGATION: A BRIEF REVIEW OF IMPORTANCE OF BIOLOGICAL EVIDENCE, Eur. Sch. J. (ESJ. 2 (2021). https://www.scholarzest.com (accessed April 22, 2025).
- [2] J. Osterburg, Criminal Investigation: A Method for Reconstructing the Past, Routledge, 2013. https://doi.org/10.4324/9781315721866.
- [3] H. Cunningham, A. Bathrick, J. Davoren, Effective Long-term Preservation of Biological Evidence, 2018.
- [4] D. Aloraer, N.H. Hassan, B. Albarzinji, W. Goodwin, Collection protocols for the recovery of biological samples, Forensic Sci. Int. Genet. Suppl. Ser. 5 (2015) e207–e209. https://doi.org/10.1016/J.FSIGSS.2015.09.083.
- [5] I. Sorokulova, E. Olsen, V. Vodyanoy, Biopolymers for sample collection, protection, and preservation, Appl. Microbiol. Biotechnol. 99 (2015) 5397–5406. https://doi.org/10.1007/S00253-015-6681-3/FIGURES/2.
- [6] H.C. Lee, C. Ladd, Preservation and Collection of Biological Evidence, Croat. Med. J. 42 (2001) 225–228. www.cmj.hr (accessed April 22, 2025).
- [7] V. Barley, Medical Malpractice: Radiotherapy, Encycl. Forensic Leg. Med. Second Ed. (2015) 494–497. https://doi.org/10.1016/B978-0-12-800034-2.00281-0.
- [8] R.J. Dinis-Oliveira, F. Carvalho, J.A. Duarte, F. Remião, A. Marques, A. Santos, T. Magalhães, Collection of biological samples in forensic toxicology, Toxicol. Mech. Methods. 20 (2010) 363–414. https://doi.org/10.3109/15376516.2010.497976.
- [9] J. Bonnet, M. Colotte, D. Coudy, V. Couallier, J. Portier, B. Morin, S. Tuffet, Chain and conformation stability of solid-state DNA: implications for room temperature storage, Nucleic Acids Res. 38 (2010) 1531–1546. https://doi.org/10.1093/NAR/GKP1060.
- [10] H.M. Lisboa, M.B. Pasquali, A.I. dos Anjos, A.M. Sarinho, E.D. de Melo, R. Andrade, L. Batista, J. Lima, Y. Diniz, A. Barros, Innovative and Sustainable Food Preservation Techniques: Enhancing Food Quality, Safety, and Environmental Sustainability, Sustain. 2024, Vol. 16, Page 8223. 16 (2024) 8223. https://doi.org/10.3390/SU16188223.
- [11] T. Mkhari, J.O. Adeyemi, O.A. Fawole, Recent Advances in the Fabrication of Intelligent Packaging for Food Preservation: A Review, Processes. 13 (2025) 539. https://doi.org/10.3390/PR13020539.
- [12] T.H. Jang, S.C. Park, J.H. Yang, J.Y. Kim, J.H. Seok, U.S. Park, C.W. Choi, S.R. Lee, J. Han, Cryopreservation and its clinical applications, Integr. Med. Res. 6 (2017) 12–18. https://doi.org/10.1016/J.IMR.2016.12.001.
 - [13] B.J. Fuller, A.Y. Petrenko, J. V. Rodriguez, A.Y. Somov, C.L. Balaban, E.E. Guibert, Biopreservation of

Egypt. J. Chem. 69, No. 2 (2026)

- Hepatocytes: Current Concepts on Hypothermic Preservation, Cryopreservation, And Vitrification, Cryo Letters. 37 (2016) 432–452.
- [14] M.S. Amiri, V. Mohammadzadeh, M.E.T. Yazdi, M. Barani, A. Rahdar, G.Z. Kyzas, Plant-Based Gums and Mucilages Applications in Pharmacology and Nanomedicine: A Review, Molecules. 26 (2021) 1770. https://doi.org/10.3390/MOLECULES26061770.
- [15] G. Abdel-Maksoud, A.-R. El-Amin, A REVIEW ON THE MATERIALS USED DURING THE MUMMIFICATION PROCESSES IN ANCIENT EGYPT, Mediterr. Archaeol. Archaeom. 11 (2011) 129–150. https://www.maajournal.com/index.php/maa/article/view/437 (accessed April 22, 2025).
- [16] A.M. Hamdani, I.A. Wani, N.A. Bhat, Sources, structure, properties and health benefits of plant gums: A review, Int. J. Biol. Macromol. 135 (2019) 46–61. https://doi.org/10.1016/J.IJBIOMAC.2019.05.103.
- [17] M. Darroudi, M.E.T. Yazdi, M.S. Amiri, Plant-Mediated Biosynthesis of Nanoparticles, in: 21st Century Nanosci. A Handb., CRC Press, 2020; pp. 1–18. https://doi.org/10.1201/9780429351525-1.
- [18] M.E. Taghavizadeh Yazdi, S. Nazarnezhad, S.H. Mousavi, M. Sadegh Amiri, M. Darroudi, F. Baino, S. Kargozar, Gum Tragacanth (GT): A Versatile Biocompatible Material beyond Borders, Molecules. 26 (2021) 1510. https://doi.org/10.3390/MOLECULES26061510.
- [19] R. Sabry, A. Sayed, I.E.T. El-Sayed, G.A. Mahmoud, Optimizing pectin-based biofilm properties for food packaging via E-beam irradiation, Radiat. Phys. Chem. 229 (2025) 112474. https://doi.org/10.1016/J.RADPHYSCHEM.2024.112474.
- [20] A. Sayed, G. Safwat, M. Abdel-raouf, G.A. Mahmoud, Alkali-cellulose/ Polyvinyl alcohol biofilms fabricated with essential clove oil as a novel scented antimicrobial packaging material, Carbohydr. Polym. Technol. Appl. 5 (2023) 100273. https://doi.org/10.1016/J.CARPTA.2022.100273.
- [21] K.Y. Perera, A.K. Jaiswal, S. Jaiswal, Biopolymer-Based Sustainable Food Packaging Materials: Challenges, Solutions, and Applications, Foods. 12 (2023) 2422. https://doi.org/10.3390/FOODS12122422.
- [22] ashgan F.M. walaa S. gado, Asmaa Sayed, Manar El-Sayed Abdel-Raouf, Gamma radiation-assisted synthesis of tea tree oil-based chitosan films for active packaging applications, Egypt. J. Chem. 68 (2025) 377–395. https://doi.org/10.1002/VNL.22226;CSUBTYPE:STRING:AHEAD.
- [23] C. Horst, C.H. Pagno, S.H. Flores, T.M.H. Costa, Hybrid starch/silica films with improved mechanical properties, J. Sol-Gel Sci. Technol. 95 (2020) 52–65. https://doi.org/10.1007/S10971-020-05234-X/FIGURES/8.
- [24] P. Chaudhary, F. Fatima, A. Kumar, Relevance of Nanomaterials in Food Packaging and its Advanced Future Prospects, J. Inorg. Organomet. Polym. Mater. 30 (2020) 5180–5192. https://doi.org/10.1007/S10904-020-01674-8/TABLES/2.
- [25] C. de Lima Barizão, M.I. Crepaldi, O. de O.S. Junior, A.C. de Oliveira, A.F. Martins, P.S. Garcia, E.G. Bonafé, Biodegradable films based on commercial κ-carrageenan and cassava starch to achieve low production costs, Int. J. Biol. Macromol. 165 (2020) 582–590. https://doi.org/10.1016/J.IJBIOMAC.2020.09.150.
- [26] N.A. Al-Tayyar, A.M. Youssef, R. Al-hindi, Antimicrobial food packaging based on sustainable Bio-based materials for reducing foodborne Pathogens: A review, Food Chem. 310 (2020) 125915. https://doi.org/10.1016/J.FOODCHEM.2019.125915.
- [27] G. Gorrasi, V. Bugatti, G. Viscusi, V. Vittoria, Physical and barrier properties of chemically modified pectin with polycaprolactone through an environmentally friendly process, Colloid Polym. Sci. 299 (2021) 429–437. https://doi.org/10.1007/S00396-020-04699-0/FIGURES/8.
- [28] A.M.A. Hasan, M. Keshawy, M.E.S. Abdel-Raouf, Atomic force microscopy investigation of smart superabsorbent hydrogels based on carboxymethyl guar gum: Surface topography and swelling properties, Mater. Chem. Phys. 278 (2022) 125521. https://doi.org/10.1016/J.MATCHEMPHYS.2021.125521.
- [29] I.E. Raschip, N. Fifere, C.D. Varganici, M.V. Dinu, Development of antioxidant and antimicrobial xanthan-based cryogels with tuned porous morphology and controlled swelling features, Int. J. Biol. Macromol. 156 (2020) 608–620. https://doi.org/10.1016/J.IJBIOMAC.2020.04.086.
- [30] E.S. Esakkimuthu, D. DeVallance, I. Pylypchuk, A. Moreno, M.H. Sipponen, Multifunctional lignin-poly (lactic acid) biocomposites for packaging applications, Front. Bioeng. Biotechnol. 10 (2022) 1025076. https://doi.org/10.3389/FBIOE.2022.1025076/BIBTEX.
- [31] X. Hou, Z. Xue, Y. Xia, Y. Qin, G. Zhang, H. Liu, K. Li, Effect of SiO2 nanoparticle on the physical and chemical properties of eco-friendly agar/sodium alginate nanocomposite film, Int. J. Biol. Macromol. 125 (2019) 1289–1298. https://doi.org/10.1016/J.IJBIOMAC.2018.09.109.
- [32] S. Estevez-Areco, L. Guz, R. Candal, S. Goyanes, Active bilayer films based on cassava starch incorporating ZnO nanorods and PVA electrospun mats containing rosemary extract, Food Hydrocoll. 108 (2020) 106054. https://doi.org/10.1016/J.FOODHYD.2020.106054.
- [33] N. Noshirvani, B. Ghanbarzadeh, R. Rezaei Mokarram, M. Hashemi, Novel active packaging based on carboxymethyl cellulose-chitosan-ZnO NPs nanocomposite for increasing the shelf life of bread, Food Packag. Shelf Life. 11 (2017) 106–114. https://doi.org/10.1016/J.FPSL.2017.01.010.
- [34] G. Sharma, S. Sharma, A. Kumar, A.H. Al-Muhtaseb, M. Naushad, A.A. Ghfar, G.T. Mola, F.J. Stadler, Guar gum and its composites as potential materials for diverse applications: A review, Carbohydr. Polym. 199 (2018) 534–545. https://doi.org/10.1016/J.CARBPOL.2018.07.053.
- [35] M. Keshawy, R. Samir, M.E.S. Abdel-Raouf, Synthesis and investigation of green hydrogels for simultaneous

- removal of mercuric cations and methylene blue from aqueous solutions, Egypt. J. Chem. 65 (2022) 325–335. https://doi.org/10.21608/EJCHEM.2021.100722.4678.
- [36] R. Ahmad, S. Haseeb, Absorptive removal of Pb2+, Cu2+ and Ni2+ from the aqueous solution by using groundnut husk modified with Guar Gum (GG): Kinetic and thermodynamic studies, Groundw. Sustain. Dev. 1 (2015) 41–49. https://doi.org/10.1016/J.GSD.2015.11.001.
- [37] J. Balachandramohan, S. Anandan, T. Sivasankar, A simple approach for the sonochemical synthesis of Fe3O4-guargum nanocomposite and its catalytic reduction of p-nitroaniline, Ultrason. Sonochem. 40 (2018) 1–10. https://doi.org/10.1016/J.ULTSONCH.2017.06.012.
- [38] V.E. Bosio, S. Basu, F. Abdullha, M. Elizabeth Chacon Villalba, J.A. Güida, A. Mukherjee, G.R. Castro, Encapsulation of Congo Red in carboxymethyl guar gum-alginate gel microspheres, React. Funct. Polym. 82 (2014) 103–110. https://doi.org/10.1016/J.REACTFUNCTPOLYM.2014.06.006.
- [39] Y.A. Arfat, M. Ejaz, H. Jacob, J. Ahmed, Deciphering the potential of guar gum/Ag-Cu nanocomposite films as an active food packaging material, Carbohydr. Polym. 157 (2017) 65–71. https://doi.org/10.1016/J.CARBPOL.2016.09.069.
- [40] A. Sayed, D.E. Hegazy, G.A. Mahmoud, Integration of ionizing radiation and nano-clay for enhancing characters of CMC-PVA/Nano-clay bio-based films, Radiochim. Acta. 113 (2025) 319–333. https://doi.org/10.1515/RACT-2024-0300
- [41] Z. Eslami, S. Elkoun, M. Robert, K. Adjallé, A Review of the Effect of Plasticizers on the Physical and Mechanical Properties of Alginate-Based Films, Molecules. 28 (2023) 6637. https://doi.org/10.3390/MOLECULES28186637.
- [42] R. Chawla, S. Sivakumar, H. Kaur, Antimicrobial edible films in food packaging: Current scenario and recent nanotechnological advancements- a review, Carbohydr. Polym. Technol. Appl. 2 (2021) 100024. https://doi.org/10.1016/J.CARPTA.2020.100024.
- [43] M. Artiga-Artigas, A. Acevedo-Fani, O. Martín-Belloso, Improving the shelf life of low-fat cut cheese using nanoemulsion-based edible coatings containing oregano essential oil and mandarin fiber, Food Control. 76 (2017) 1–12. https://doi.org/10.1016/J.FOODCONT.2017.01.001.
- [44] J.F. Islas, E. Acosta, Z. G-Buentello, J.L. Delgado-Gallegos, M.G. Moreno-Treviño, B. Escalante, J.E. Moreno-Cuevas, An overview of Neem (Azadirachta indica) and its potential impact on health, J. Funct. Foods. 74 (2020) 104171. https://doi.org/10.1016/J.JFF.2020.104171.
- [45] D. Bhatnagar, S.P. mcCormick, The inhibitory effect of neem (Azadirachta indica) leaf extracts on aflatoxin synthesis inAspergillus parasiticus, J. Am. Oil Chem. Soc. 65 (1988) 1166–1168. https://doi.org/10.1007/BF02660575.
- [46] M.M. Khan, H. Zubairy, Mycoses. Part I: antimycotic effect of Azadirachta indica on Candida albicans., Hamdard Med. 41 (1998) 33–34. https://www.cabidigitallibrary.org/doi/full/10.5555/19991202156 (accessed April 22, 2025).
- [47] P.O. Okemo, S.C. Chhabra, W. Fabry, The kill kinetics of Azadirachta indica A. JUSS. (meliaceae) extracts on Staphylococcus aureus, Escherichia coli, Pseudomonas aeruginosa and Candida albicans, African J. Sci. Technol. Sci. Eng. Ser. 2 (2001) 113–118. https://www.researchgate.net/publication/237801524 (accessed April 22, 2025).
- [48] N. Bohra, D. Purohit, Effect of some aqueous plant extracts on toxigenic strain of Aspergillus flavus., Adv. Plant Sci. 15 (2002) 103–106. https://www.cabidigitallibrary.org/doi/full/10.5555/20023110889 (accessed April 22, 2025).
- [49] V. Natarajan, P. V. Venugopal, T. Menon, EFFECT OF AZADIRACHTA INDICA (NEEM) ON THE GROWTH PATTERN OF DERMATOPHYTES, Indian J. Med. Microbiol. 21 (2003) 98–101. https://doi.org/10.1016/S0255-0857(21)03129-7.
- [50] D.A. Mahmoud, N.M. Hassanein, K.A. Youssef, M.A. Abou Zeid, Antifungal activity of different neem leaf extracts and the nimonol against some important human pathogens, Brazilian J. Microbiol. 42 (2011) 1007–1016. https://doi.org/10.1590/S1517-83822011000300021.
- [51] P. Senthilkumar, S. Rashmitha, P. Veera, C.V. Ignatious, C. Saipriya, A. V Samrot, Antibacterial Activity of Neem Extract and its Green Synthesized Silver Nanoparticles against Pseudomonas aeruginosa, J. PurE Appl. Microbiol. 12 (2018) 969–974. https://doi.org/10.22207/JPaM.12.2.60.
- [52] S. Kaur, P. Sharma, A. Bains, P. Chawla, K. Sridhar, M. Sharma, B.S. Inbaraj, Antimicrobial and Anti-Inflammatory Activity of Low-Energy Assisted Nanohydrogel of Azadirachta indica Oil, Gels. 8 (2022) 434. https://doi.org/10.3390/GELS8070434.
- [53] M.G.A. Vieira, M.A. Da Silva, L.O. Dos Santos, M.M. Beppu, Natural-based plasticizers and biopolymer films: A review, Eur. Polym. J. 47 (2011) 254–263. https://doi.org/10.1016/J.EURPOLYMJ.2010.12.011.
- [54] S. Jafarzadeh, A.K. Alias, F. Ariffin, S. Mahmud, Physico-mechanical and microstructural properties of semolina flour films as influenced by different sorbitol/glycerol concentrations, Int. J. Food Prop. 21 (2018) 983–995. https://doi.org/10.1080/10942912.2018.1474056.
- [55] J.O. Adeyemi, O.A. Fawole, Metal-Based Nanoparticles in Food Packaging and Coating Technologies: A Review, Biomolecules. 13 (2023) 1092. https://doi.org/10.3390/BIOM13071092.
- [56] A.A. Arman Alim, S.S. Mohammad Shirajuddin, F.H. Anuar, A Review of Nonbiodegradable and Biodegradable Composites for Food Packaging Application, J. Chem. 2022 (2022) 7670819. https://doi.org/10.1155/2022/7670819.
- [57] N. Abdullahi, Advances in food packaging technology-a review, J. Postharvest Technol. 06 (2018) 55–64. https://www.researchgate.net/profile/Nura-Abdullahi/publication/331414348_Advances_in_food_packaging_technology-A_review/links/5c7863f4458515831f781d82/Advances-in-food-packaging-technology-A-review.pdf (accessed June 2, 2025).

- [58] A. Krishnamurthy, P. Amritkumar, Synthesis and characterization of eco-friendly bioplastic from low-cost plant resources, SN Appl. Sci. 1 (2019) 1–13. https://doi.org/10.1007/S42452-019-1460-X.
- [59] G. El Fawal, H. Hong, X. Song, J. Wu, M. Sun, ... C.H.-, Fabrication of antimicrobial films based on hydroxyethylcellulose and ZnO for food packaging application, Food Packag. Shelf Life. 23 (2020) 1–7. https://www.sciencedirect.com/science/article/pii/S2214289419306416?casa_token=u2pR4YLizxEAAAAA:qKydG VirmeNrEqh9JVhPZRpFkgoqiqt6CT25YghBK9FxfmQO-86C0moOWgXYuzvleCO3-9evuJhFlg (accessed June 2, 2025).
- [60] H. Yousefi, H.M. Su, S.M. Imani, K. Alkhaldi, C.D. Filipe, T.F. Didar, Intelligent food packaging: A review of smart sensing technologies for monitoring food quality, ACS Sensors. 4 (2019) 808–821. https://doi.org/10.1021/ACSSENSORS.9B00440.
- [61] S. Ghosh, T.B.-I.J. of B. Macromolecules, U. 2025, Neem gum and its derivatives as potential polymeric scaffold for diverse applications: a review, Nternational J. Biol. Macromol. 310 (2025) 143012. https://www.sciencedirect.com/science/article/pii/S0141813025035640?casa_token=iBRUuFxa4cUAAAAA:reThr1 WKfXHDn0SMqMOh2m14b8IvjS1NC9UEZOMGzKp9BcnkOkrs4Su6CDB7QsJOCZ-HHB5GlU-zsg (accessed June 2, 2025).
- [62] G. Sangeetha, S. Rajeshwari, R.V. Bulletin, Green synthesis of zinc oxide nanoparticles by aloe barbadensis miller leaf extract: Structure and optical properties, Mater. Res. Bull. 46 (2011) 2560–2566. https://www.sciencedirect.com/science/article/pii/S0025540811003734?casa_token=vP9I_w4hKfMAAAAA:OHg7q MgCsIarJMgAXtJUqMqn3IyH1hH65BtsF_Lrbrlmalp1bFz9O6RsQzeeg1pzv7nLiGOCXZ2VwA (accessed June 2, 2025).
- [63] M.E.-S. Abdel-Raouf, M. Keshawy, A. Sayed, A.M.A. Hasan, Application of Guar Gum and its Derivatives in the Biomedical Field2025) .2025 (). https://doi.org/10.1201/9780367694265-EPPMPT14-1.
- [64] A. Hasan, M. Keshawy, M.A.-R.- And, Atomic force microscopy investigation of smart superabsorbent hydrogels based on carboxymethyl guar gum: Surface topography and swelling properties, Mater. Chem. Physics (2022) 278. 125521. https://www.sciencedirect.com/science/article/pii/S0254058421013043?casa_token=hig7pj6oZRUAAAAA:5J1L_O WBESmpGLKFvYziISFA-T3EaJcttz_sgCDq-8FiJ3vFGIr_xQBrQ6W4x_f-VjGsJZzCMNdmnQ (accessed June 2, 2025).
- [65] A. Sayed, M. Mohamed, ... M.A.-, Radiation synthesis of green nanoarchitectonics of guar gum-pectin/polyacrylamide/zinc oxide superabsorbent hydrogel for sustainable agriculture, J. Inorg. Organomet. Polym. Mater. 32 (2022) 4589–4600. https://doi.org/10.1007/S10904-022-02465-Z.+(2022)+32:4589.
- T.R. Bhardwaj, M. Kanwar, R. Lal, A. Gupta, Natural gums and modified natural gums as sustained-release carriers Drug Dev. Ind. 26 (2000) 1025–1038. https://doi.org/10.1081/DDC-100100266.
- [67] A. Jeżo, F. Poohphajai, R.H. Diaz, G.K.- Materials, Incorporation of Nano-Zinc Oxide as a Strategy to Improve the Barrier Properties of Biopolymer–Suberinic Acid Residues Films: A Preliminary Study, Materials (Basel). 17 (2024) 3868–3884. https://doi.org/10.20944/PREPRINTS202406.1807.V1.
- [68] S. Azlin-Hasim, M.C. Cruz-Romero, E. Cummins, J.P. Kerry, M.A. Morris, The potential use of a layer-by-layer strategy to develop LDPE antimicrobial films coated with silver nanoparticles for packaging applications, J. Colloid Interface Sci. 461 (2016) 239–248. https://doi.org/10.1016/J.JCIS.2015.09.021.
- [69] S.L. Duraikkannu, R. Castro-Muñoz, A. Figoli, A review on phase-inversion technique-based polymer microsphere fabrication, Colloid Interface Sci. Commun. 40 (2021) 100329. https://doi.org/10.1016/J.COLCOM.2020.100329.
- [70] K. Elumalai, S. Velmurugan, Green synthesis, characterization and antimicrobial activities of zinc oxide nanoparticles from the leaf extract of Azadirachta indica (L.), Appl. Surf. Sci. 345 (2015) 329–336. https://doi.org/10.1016/J.APSUSC.2015.03.176.
- [71] A. Ali, M.A. Shahid, M.D. Hossain, M.N. Islam, Antibacterial bi-layered polyvinyl alcohol (PVA)-chitosan blend nanofibrous mat loaded with Azadirachta indica (neem) extract, Int. J. Biol. Macromol. 138 (2019) 13–20. https://doi.org/10.1016/J.IJBIOMAC.2019.07.015.
- [72] P. Bhadra, M.K. Mitra, G.C. Das, R. Dey, S. Mukherjee, Interaction of chitosan capped ZnO nanorods with Escherichia coli, Mater. Sci. Eng. C. 31 (2011) 929–937. https://doi.org/10.1016/J.MSEC.2011.02.015.
- [73] R. Subapriya, S.N.-C.M. Chemistry-Anti, undefined 2005, Medicinal properties of neem leaves: a review, Benthamdirect.ComR Subapriya, S NaginiCurrent Med. Chem. Agents, 2005•benthamdirect.Com156–149 (2005) 5... https://doi.org/10.2174/1568011053174828.
- [74] U. Amin, M.K.I. Khan, A.A. Maan, A. Nazir, S. Riaz, M.U. Khan, M. Sultan, P.E.S. Munekata, J.M. Lorenzo, Biodegradable active, intelligent, and smart packaging materials for food applications, Food Packag. Shelf Life. 33 (2022) 100903. https://doi.org/10.1016/J.FPSL.2022.100903.
- [75] C. Antonino, G. Difonzo, M. Faccia, F. Caponio, Effect of edible coatings and films enriched with plant extracts and essential oils on the preservation of animal-derived foods, J. Food Sci. 89 (2024) 748–772. https://doi.org/10.1111/1750-3841.16894;WEBSITE:WEBSITE:IFT;REQUESTEDJOURNAL:JOURNAL:17503841;WGROUP:STRING:PUBL ICATION.
- [76] S. Guo, Y. Guo, X. Yang, X. Wang, R. Zhang, S. Wang, M. Li, A review on polymer packaging by polysaccharide-based nanocomposite films: crucial role of nanofillers and future application trends, J. Food Meas. Charact. 19 (2025)

- 2987-3004. https://doi.org/10.1007/S11694-025-03199-5.
- [77] T. Gasti, V.D. Hiremani, S.S. Kesti, V.N. Vanjeri, N. Goudar, S.P. Masti, S.C. Thimmappa, R.B. Chougale, Physicochemical and Antibacterial Evaluation of Poly (Vinyl Alcohol)/Guar Gum/Silver Nanocomposite Films for Food Packaging Applications, J. Polym. Environ. 29 (2021) 3347–3363. https://doi.org/10.1007/S10924-021-02123-4/METRICS.
- [78] E. Kirtil, A. Aydogdu, T. Svitova, C.J. Radke, Assessment of the performance of several novel approaches to improve physical properties of guar gum based biopolymer films, Food Packag. Shelf Life. 29 (2021) 100687. https://doi.org/10.1016/J.FPSL.2021.100687.
- [79] D.N. Iqbal, S. Shafiq, S.M. Khan, S.M. Ibrahim, S.A. Abubshait, A. Nazir, M. Abbas, M. Iqbal, Novel chitosan/guar gum/PVA hydrogel: Preparation, characterization and antimicrobial activity evaluation, Int. J. Biol. Macromol. 164 (2020) 499–509. https://doi.org/10.1016/J.IJBIOMAC.2020.07.139.
- [80] N.A. Aal, F. Al-Hazmi, A.A. Al-Ghamdi, A.A. Al-Ghamdi, F. El-Tantawy, F. Yakuphanoglu, Novel rapid synthesis of zinc oxide nanotubes via hydrothermal technique and antibacterial properties, Spectrochim. Acta Part A Mol. Biomol. Spectrosc. 135 (2015) 871–877. https://doi.org/10.1016/J.SAA.2014.07.099.
- [81] S. Rahman, A. Konwar, G. Majumdar, D. Chowdhury, Guar gum-chitosan composite film as excellent material for packaging application, Carbohydr. Polym. Technol. Appl. 2 (2021) 100158. https://doi.org/10.1016/J.CARPTA.2021.100158.
- [82] H.M. Shaikh, A. Anis, A.M. Poulose, N.A. Madhar, S.M. Al-Zahrani, Date-Palm-Derived Cellulose Nanocrystals as Reinforcing Agents for Poly(Vinyl Alcohol)/Guar-Gum-Based Phase-Separated Composite Films, Nanomaterials. 12 (2022) 1104. https://doi.org/10.3390/NANO12071104/S1.
- [83] Y. Meng, Y. Cao, K. Xiong, L. Ma, W. Zhu, Z. Long, C. Dong, Effect of cellulose nanocrystal addition on the physicochemical properties of hydroxypropyl guar-based intelligent films, Membranes (Basel). 11 (2021) 242. https://doi.org/10.3390/MEMBRANES11040242/S1.
- [84] D. Jussen, S. Sharma, J.K. Carson, K.L. Pickering, Preparation and tensile properties of guar gum hydrogel films, Polym. Polym. Compos. 28 (2020) 180–186. https://doi.org/10.1177/0967391119867560/ASSET/CDCF5634-5CBD-416F-8448-9B3541468BD3/ASSETS/IMAGES/LARGE/10.1177 0967391119867560-FIG8.JPG.
- [85] N. Thombare, U. Jha, S. Mishra, M.Z. Siddiqui, Guar gum as a promising starting material for diverse applications: A review, Int. J. Biol. Macromol. 88 (2016) 361–372. https://doi.org/10.1016/J.IJBIOMAC.2016.04.001.
- [86] A.C. Alavarse, E.C.G. Frachini, R.L.C.G. da Silva, V.H. Lima, A. Shavandi, D.F.S. Petri, Crosslinkers for polysaccharides and proteins: Synthesis conditions, mechanisms, and crosslinking efficiency, a review, Int. J. Biol. Macromol. 202 (2022) 558–596. https://doi.org/10.1016/J.IJBIOMAC.2022.01.029.
- [87] H. Valadbeigi, N. Sadeghifard, V.H. Kaviar, M.H. Haddadi, S. Ghafourian, A. Maleki, Effect of ZnO nanoparticles on biofilm formation and gene expression of the toxin-antitoxin system in clinical isolates of Pseudomonas aeruginosa, Ann. Clin. Microbiol. Antimicrob. 22 (2023) 1–8. https://doi.org/10.1186/S12941-023-00639-2/TABLES/3.
- [88] S. Shankar, J.W. Rhim, Effect of types of zinc oxide nanoparticles on structural, mechanical and antibacterial properties of poly(lactide)/poly(butylene adipate-co-terephthalate) composite films, Food Packag. Shelf Life. 21 (2019) 100327. https://doi.org/10.1016/J.FPSL.2019.100327.
- [89] V. Singh, L.M. Dwivedi, K. Baranwal, S. Asthana, S. Sundaram, Oxidized guar gum—ZnO hybrid nanostructures: synthesis, characterization and antibacterial activity, Appl. Nanosci. 8 (2018) 1149–1160. https://doi.org/10.1007/S13204-018-0747-3/TABLES/3.